

Asset Characterization Using Automated Methods



April 2025
Final Report

Project number TR202311
MoDOT Research Report number cmr 25-005

PREPARED BY:

Sungyop Kim

Donald Baker

Jejung Lee

Aaron Sprague

Charles Mwaipopo

University of Missouri-Kansas City and Water Resources Solutions, LLC

PREPARED FOR:

Missouri Department of Transportation

Construction and Materials Division, Research Section

Technical Report Documentation Page

1. Report No. cmr 25-005	2. Government Accession No.	3. Recipient's Catalog No.	
4. Title and Subtitle Asset Characterization Using Automated Methods		5. Report Date March 2025 Published: April 2025	
		6. Performing Organization Code	
7. Author(s) Sungyop Kim, 0000-0002-1784-1813, https://orcid.org/0000-0002-1784-1813 Donald Baker, 0009-0005-9233-2807, https://orcid.org/0009-0005-9233-2807 Jejung Lee, 0000-0002-8253-3710, https://orcid.org/0000-0002-8253-3710 Aaron Sprague, 0009-0002-7723-801X, https://orcid.org/0009-0002-7723-801X Charles Mwaipopo, 0009-0006-3812-4617, https://orcid.org/0009-0006-3812-4617		8. Performing Organization Report No.	
9. Performing Organization Name and Address University of Missouri – Kansas City 5000 Holmes St. Kansas City, MO 64110 Water Resources Solutions, LLC 5000 W 95th St., #290 Prairie Village, KS 66207		10. Work Unit No. (TRAIS)	
		11. Contract or Grant No. MoDOT project #TR202311	
12. Sponsoring Agency Name and Address Missouri Department of Transportation (SPR-B) Construction and Materials Division P.O. Box 270 Jefferson City, MO 65102		13. Type of Report and Period Covered Final Report (June 2023-March 2025)	
		14. Sponsoring Agency Code	
15. Supplementary Notes Conducted in cooperation with the U.S. Department of Transportation, Federal Highway Administration. MoDOT research reports are available in the Innovation Library at https://www.modot.org/research-publications .			
16. Abstract Increasing and intensifying flood events pose serious challenges to highway agencies in maintaining water crossing assets and assessing potential flood hazards. This project aimed to develop an automated flood risk assessment program for small water crossing assets, focusing on culverts with less than a 20-foot span not listed in the 2023 National Bridge Inventory (NBI). Information on such small assets is often limited and not readily available. Using a Geographic Information System (GIS), the project identified potential non-NBI water crossing sites and conducted field surveys to collect the asset information on Missouri's highways. Based on the field survey data, the project developed a GIS-based flood risk assessment tool for small water crossing assets, called the Missouri Automated Culvert Analysis Tool (MoACAT) QGIS Plugin, using publicly available high-resolution Light Detection and Ranging (LiDAR) data. The tool was built with Python scripts that process four sequential steps on the Quantum Geographic Information System (QGIS), the most popular non-proprietary open-source GIS software program. The project conducted a pilot study of culverts in Cass County, Missouri. The plugin hydraulic results were compared against HEC-RAS 2D modeling results. The results indicate that the tool has the potential to identify small water crossing assets and predict flood overtopping efficiently.			
17. Key Words Flood; Risk assessment; LiDAR; Water crossings		18. Distribution Statement No restrictions. This document is available through the National Technical Information Service, Springfield, VA 22161.	
19. Security Classification (of this report) Unclassified	20. Security Classification (of this page) Unclassified	21. No. of Pages 55	22. Price

Asset Characterization Using Automated Methods

By

Sungyop Kim, Ph.D.

Jejung Lee, Ph.D.

Charles Mwaipopo

University of Missouri – Kansas City

Donald Baker, P.E.

Aaron Sprague, E.I.

Water Resources Solutions, LLC

Prepared for

Missouri Department of Transportation

March 2025

Final Report

Copyright

Authors herein are responsible for the authenticity of their materials and for obtaining written permissions from publishers or individuals who own the copyright to any previously published or copyrighted material used herein.

Disclaimer

The findings, interpretations, and conclusions expressed in this document are those of the author(s) and do not necessarily reflect the views of the Missouri Department of Transportation.

Acknowledgments

The project team appreciates the Missouri Department of Transportation (MoDOT) for funding the project. Special thanks for the guidance and inputs provided by Chris Engelbrecht, Director of the Safety and Emergency Management Division, Brent Schulte, Senior Research Analyst of MoDOT Research, and Jen Harper, Director of MoDOT Research.

Table of Contents

Executive Summary.....	1
Chapter 1. Introduction	3
1.1 Project Overview	3
1.2 Literature Review	4
1.2.1 Flood Risk Assessment	4
1.2.2 LiDAR for Asset Management	5
1.2.3 Use of LiDAR among State Highway Agencies	6
Chapter 2. Survey Study on Water Crossing Assets.....	8
2.1 Water Crossing Asset Data Development	8
2.2 Surveyed Small Water Crossing Assets.....	12
Chapter 3. Hydraulic Model Development for Flood Risk Assessment	14
3.1 Model Workflow Overview	14
3.1.1 Process Outline	14
3.1.2 Process Description.....	15
3.2 Hydrology	17
3.2.1 Methodology.....	17
3.2.2 Parameter Estimation	18
3.3 Width Regression	18
3.3.1 Methodology.....	18
3.3.2 Correlation Results.....	19
3.4 Culvert Hydraulics.....	19
3.4.1 Methodology.....	20
3.4.2 Parameter estimation	21
3.5 Plugin development.....	21
3.6 Assessment of Hydraulic Model Results.....	22
Chapter 4. Conclusions and Recommendations	24
References	26
Appendix: User Manual of the Missouri Automated Culvert Analysis Tool (MoACAT) Plugin	1
Introduction.....	1
Part 1	1
System Requirements.....	1
Required Inputs	2
Installation Guide.....	3

Part 2 Example Walkthrough..... 5

Processing Tools 7

List of Tables

Table 2-1. Characteristics of Water Crossing Assets.....	13
Table 3-1. Correlation Matrix.....	19
Table 3-2. GIS Plugin Validation Results	22

List of Figures

Figure 2-1. Bridge and Culvert Locations of the 2023 National Bridge Inventory (NBI) Data	8
Figure 2-2. Potential Locations of Non-NBI Assets in the Kansas City Metro Counties.....	9
Figure 2-3. Water Crossing Site Screening using Google Maps and Google Earth	10
Figure 2-4. Surveying the Water Crossing Assets	10
Figure 2-5. Examples of Unsurveyable Non-NBI Water Crossing Sites.....	11
Figure 2-6. Visited and Surveyed Water Crossing Assets in the Kansas City Metro Counties	11
Figure 3-1. Process Flow Chart.....	15
Figure 3-2. HDS 5 Outlet Control Flow Types.....	21
Figure 3-3. Example of HEC-RAS Cross-Section Showing the Culvert Opening	22

List of Equations

Equation 3-1. Direct Runoff Depth for $P \geq I_a$ ($Q=0$ if $P < I_a$)	17
Equation 3-2. Initial Abstractions	17
Equation 3-3. Time of Concentration	18
Equation 3-4. Unsubmerged Inlet Control.....	20
Equation 3-5. Submerged Inlet Control	20

List of Abbreviations and Acronyms

DOA	Department of Agriculture
DEM	Digital Elevation Model
DOT	Department of Transportation
DSM	Digital Surface Model
EPA	Environmental Protection Agency
FEMA	Federal Emergency Management Agency
FHWA	Federal Highway Administration
FIM	Flood Inundation Mapping
GIS	Geographic Information System
HEC-RAS	Hydrologic Engineering Center's River Analysis System
LiDAR	Light Detection and Ranging
LWC	Low Water Crossing
MoACAT	Missouri Automated Culvert Analysis Tool
MoDOT	Missouri Department of Transportation
MSDIS	Missouri Spatial Data Information Service
NBI	National Bridge Inventory
NEH	National Engineering Handbook
NFHL	National Flood Hazard Layer
NLCD	National Land Cover Database
NRCS	Natural Resources Conservation Service
NWS	National Weather Service
QGIS	Quantum Geographic Information System
SSURGO	Soil Survey Geographic Database
USACE	United States Army Corps of Engineers
USGS	United States Geological Survey
WQS	Water Quality Standard

Executive Summary

Floods are frequent, hazardous, and costly natural disasters with significant societal consequences. Due to climate change, the number and intensity of extreme flood events are expected to increase significantly in the coming decades. Floods have broad impacts on the built environment, including highway infrastructure. Flood impacts on highway infrastructure include damage to the infrastructure itself, safety concerns for the public using the infrastructure during flood events, and significant disruptions to transportation networks and traffic flows near rivers and streams during flood events. Thus, highway agencies face increasing challenges in maintaining and monitoring water crossing assets and assessing flood hazard risks of those assets.

This project aimed to develop an automated flood risk assessment tool using existing Light Detection and Ranging (LiDAR) data for small water crossing assets on Missouri's highways not listed in the 2023 National Bridge Inventory (NBI) database. LiDAR is a remote sensing technology where laser pulses are emitted at object surfaces to create 3D point cloud representations of the objects. Thus, generating high-resolution 3D models or Geographic Information System (GIS) mappings such as Digital Elevation Models (DEM) and Digital Surface Models (DSM). LiDAR data are increasingly available and have been used by many state highway agencies for various purposes, including highway, infrastructure, natural, topographic, and terrain data collection and asset management. The project employed readily available 6.56-foot (or two-meter) resolution topographic LiDAR data from the Missouri Spatial Data Information Service (MSDIS).

The project focused on small water crossing assets with spans under 20 feet that were not listed in the 2023 NBI data. Information on such small assets is often limited and not readily available. Thus, the project used GIS to identify potential non-NBI water crossing sites and conducted field surveys to collect the asset information. The project focused on box culverts, the most widely found type of small water crossing asset. Focusing on non-NBI culverts, the project developed a GIS-based flood risk assessment tool or the Missouri Automated Culvert Analysis Tool (MoACAT), using the readily available high-resolution LiDAR data. The tool was built as a plugin with Python scripts that process four sequential steps in the Quantum Geographic Information System (QGIS), the most popular non-proprietary open-source GIS software program. The choice to use QGIS was made to ensure easy and affordable testing and implementation. The four steps involve 1) DEM hydro-conditioning and stream creation to determine runoff flow directions, 2) culvert location identification with elevation attributes, 3) culvert hydrology computations for peak design storm discharge, and 4) culvert hydraulic computations for water overtopping.

The project conducted a pilot study using surveyed culverts in Cass County, Missouri, the location of most box culverts surveyed. The MoACAT hydraulic results were compared against HEC-RAS 2D modeling results. The results indicate that the tool has the potential to identify small water crossing assets and predict flood overtopping efficiently. The project developed a

step-by-step manual of the flood risk assessment tool with a sample dataset based on the assets used for the pilot study.

The MoACAT program has significant potential. It should be able to help the Missouri Department of Transportation (MoDOT) identify and manage small assets on Missouri's highways. The outputs will assist MoDOT in assessing small, flood-prone assets. This information can be used for highway and emergency management, prioritizing highway infrastructure investment to safeguard water crossing infrastructure and road users, providing efficient, reliable, and safe transportation networks, and ensuring efficient water crossing asset management.

Chapter 1. Introduction

1.1 Project Overview

Floods are destructive and have significant societal impacts. In the U.S., the number of fatalities directly related to floods between 2010-2024 was 1,560 (NWS, n.d.) and the annual financial loss related to flooding is estimated to be \$32.1 billion (Wing et al. 2022). Increases in the frequency and intensity of extreme precipitation events and the risk of flooding are expected in the coming decades (Tabari 2020). Wing et al. (2022) projected a 26.4% increase in flood risk by 2050. Regional variations in flood event type exist in the U.S. (EPA, n.d.). The Midwest and Northeast experienced more significant increases in the frequency and magnitude of river and stream floodings over the past decades (EPA, n.d.; Mallakpour and Villarini 2015).

Floods have broad societal impacts, including damaging effects on road safety and highway infrastructure. Floods can also significantly disrupt traffic flows (Pregolato et al. 2017). Therefore, flood mitigation measures to safeguard transportation assets have been increasingly critical in the era of climate change, with more frequent and intense flood events. The U.S. Department of Transportation (USDOT) states that "to protect the integrity of the nation's transportation system and the people it serves, it is essential to manage and reduce flood risk when taking actions to plan, design, maintain, and repair our transportation system." (USDOT, n.d., 2). The first step in managing flood risk in transportation may be systematic flood risk assessment.

This project aimed to develop a hydraulic modeling system to assess the flood risks of Missouri's highway assets, focusing on water crossing assets fewer than 20 feet in span that are not listed in the 2023 National Bridge Inventory (NBI) database (FHWA, n.d.). The NBI data maintained by the Federal Highway Administration (FHWA) includes information on over 600,000 major US highway bridges and culverts, including 24,617 assets in Missouri. The water crossing assets listed in the NBI have legislative reporting requirements on their conditions to ensure the structural integrity and safety of the assets. However, there are still numerous small water crossing assets that are not listed in the NBI. The information on those non-NBI assets is often limited or not readily available, even though they are also important highway assets that contribute to surface transportation systems. Those small non-NBI assets also need to be maintained to cope with various risks, including floods.

This project developed an automated hydraulic modeling system to identify potential non-NBI assets and the flood risk assessment of those assets using publicly available data sources. The project conducted spatial analyses for system development using Light Detection and Ranging (LiDAR) data and Geographic Information System (GIS). Field surveys were conducted to identify the non-NBI asset locations on MoDOT highways and measure their characteristics. A critical element of the modeling system is utilizing high-resolution LiDAR data and hydraulic modeling approaches that are readily available so the system can be cost-effective, accurate, reliable, and user-friendly. The project developed an easy-to-implement GIS-based hydraulic modeling system for flood risk assessment for small assets. Specifically, the project developed a

Python plugin that works with Quantum Geographic Information System (QGIS), a popular non-proprietary open-source GIS software, for automated processing of flood risk assessment.

1.2 Literature Review

The following literature review discusses current research and state-of-the-practice on flood risk assessment, the use of LIDAR for transportation asset management, and the use of LIDAR within State Agencies.

1.2.1 Flood Risk Assessment

More frequent and intense flood events require more attention to flood risk assessment. Flood risk assessment involves determining the likelihood (or probability) of potential flood hazards and providing alternatives to mitigate flood impacts. The assessment is comprised of four primary elements (flood hazards, economic exposure, vulnerability, and mitigation strategies) and considers various factors, such as rainfall, land slopes, land use type, vegetation, soil characteristics, and drainage levels (Wang et al. 2015; Xu et al. 2018). Flood hazards are typically identified via flood hazard and inundation maps. The likelihood and severity of flooding, considering depth, flow velocity, and discharge, help forecast the flood hazard. Hydrodynamic modeling tools such as the U.S. Army Corps of Engineers' (USACE) Hydrologic Engineering Center River Analysis System (HEC-RAS) modeling software (USACE, n.d.), DHI's MIKE software (DHI, n.d.), the Federal Emergency Management Agency (FEMA)'s National Flood Hazard Layer (NFHL) (FEMA, n.d.), or the U.S. Geological Survey (USGS)'s Flood Inundation Mapping (FIM) Program, (USGS, n.d.) are commonly used to develop and access flood hazard and inundation maps.

Flood hazard mapping plays a crucial role in evaluating flood risks. It forecasts the extent and depth of flood waters through hydrodynamic models. Thus, it is sometimes referred to as flood inundation or flood susceptibility mapping. A key application of this mapping is to measure risks associated with flood events of specific return periods (e.g., a 100-year event), offering essential risk-based information regarding infrastructure planning and land use. It can also forecast surface water levels during storm events. A flood inundation model requires the hydrological and hydraulic system and boundary conditions such as upstream inflow and precipitation. The most conventional flood forecasting and inundation mapping program is HEC-RAS, developed by the USACE. The HEC-RAS system contains the following river analysis components: 1) one-dimensional steady flow water surface profile computations, 2) one-dimensional and/or two-dimensional unsteady flow simulation, 3) quasi unsteady or fully unsteady flow movable boundary sediment transport computations (1D and 2D), and 4) one-dimensional water quality analysis. HEC-RAS also has an extensive spatial data integration and mapping system, such as HEC-RAS Mapper (USACE, n.d.) and HEC-GeoRAS (USACE, n.d.), a GIS extension for two-dimensional floodplain modeling.

Kolakovic et al. (2021) employed stream channel models derived from terrestrial LiDAR integrated within HEC-RAS to conduct hydraulic flood modeling for the Danube River in Southeast Europe. Bruno et al. (2022) used HEC-RAS to identify flood-prone areas for 5, 10, 50,

and 100 year storms in Campo Grande, Mato Grosso do Sul in Brazil. Although HEC-RAS serves as a valuable tool for hydrology and flood modeling, it demands a substantial amount of input data, including stream geometry, flow data, and details about flow regimes. The use of LiDAR-based digital elevation models with resolutions under 3.28 feet (one meter) can result in billion-cell datasets for watershed-scale analysis, resulting in high computational costs. However, with improved computational capabilities, these simulations have become more accessible, and a growing number of states, twenty-nine as of 2021 (Barclay and Smith 2021), have begun utilizing LiDAR datasets for floodplain modeling.

The 100-year floodplain has been historically adopted as the primary tool for determining the flood risks in the flood risk assessment. As defined by FEMA (2017), communities in a 100-year floodplain have a one percent chance of flooding in any given year. However, Patterson and Doyle (2009) and Brody et al. (2012) reported that the 100-year floodplain may be inadequate for delineating flood risks. Patterson and Doyle (2009) showed a significant increase in flood exposure outside the 100-year floodplain in North Carolina. Brody et al. (2012) showed that in southwest Texas the highest concentration of economic losses corresponded to the floodplain boundary. However, they also found significant areas of damage pushed outward into surrounding neighborhoods that did not lie within the 100-year floodplain. One possible explanation for the larger than expected damage area is the use of FEMA flood maps that are not regularly updated. Gallagher (2014) studied the flood insurance take-up between flooded and non-flooded communities. The study showed that some communities still relied on flood maps created in the 1970s and the early 1980s, which do not reflect current flood events. The other explanation is that 100-year flooding events occur more frequently than expected, due to climate change. Boumis et al. (2023) predicted that 100-year flooding could occur every year by the end of the century in most coastal cities under the current climate change scenario. Therefore, relying solely on FEMA's, often not updated, 100-year flood zones to determine flood risks may not be sufficient to assess flood risks. This may also be true for highway infrastructure, including water crossing assets.

1.2.2 LiDAR for Asset Management

LiDAR data has emerged as an important source for various spatial data analyses, including flood risk analyses. LiDAR is a remote sensing method utilized to construct topography through laser pulses. LiDAR instruments record how emitted light reflects off the surrounding terrain and transforms the returned signals into a point cloud. This point cloud can be converted into digital elevation models (DEMs) representing ground elevations and digital surface models (DSMs) capturing the natural and built features.

LiDAR data can be gathered from aerial devices situated on airplanes, which can cover expansive geographical regions; however, the resolution of the LiDAR data tends to be lower for these aerial devices due to the fewer laser pulses per spatial unit (Young et al. 2010). LiDAR data can also be acquired using terrestrial devices, like those mounted on moving vehicles or carried in backpacks (Williams et al. 2013). Since these ground-based LiDAR systems are closer

to the earth's surface and typically operate at a slower pace while collecting data, the resulting point clouds have a higher resolution, leading to more detailed DEMs (Wang et al. 2013).

High resolution DEMs are crucial for accurately analyzing flooding and rising water levels in streams because microtopographic elements affect flow paths, velocities, and the intensity of flooding (Ramachandran et al. 2023). Amatya et al. (2013) re-conditioned a surface elevation model using LiDAR DEM to minimize discontinuous streams due to bridges and culverts. Another study on LiDAR-based surface models for highway drainage (Hans et al. 2003) reported that using high-resolution LiDAR data can significantly impact highway projects in flood plains with relatively flat terrain, where even a small change can substantially impact drainage patterns. LiDAR has become the predominant source of topographic data for floodplain delineation and flood risk assessment.

LiDAR is also a cost-effective tool for transportation asset/inventory management compared to traditional survey methods (Guan et al. 2016; Sairam et al. 2016). In many studies, LiDAR has demonstrated the capacity to inventory various types of assets. For example, power lines (Ussyshkin et al. 2011), traffic signs and pavement markings (Li et al. 2023), drainage channels (Gharaibeh et al. 2023), guardrails (Yue et al. 2021), sidewalks (Hou and Ai, 2020), retro-reflectivity of traffic signs (Ai and Tsai 2016), rail tracks (Strong and Holt 2011), vegetation, vertical bridge clearance, and bridge condition (Gargoum et al. 2018). However, Li et al. (2023) found LiDAR was ineffective in picking up the color and location of traffic signs, even though inventorying of scanned traffic control devices was mainly effective. Martin et al. (2020) investigated if replacing traditional survey methods with LiDAR was cost-effective for the Oregon Department of Transportation (ODOT). Despite the initial investment required to utilize LiDAR, this study found that when replacing traditional survey methods with LiDAR, for every dollar invested in LiDAR, a \$2 return was produced for ODOT. The study found LiDAR more flexible than other traditional survey methods for asset inventory because of its many potential uses and its ability to withstand high speeds and various weather conditions. In sum, existing studies found LiDAR to be an effective, efficient, and versatile technology for DOTs to use for asset inventory purposes.

1.2.3 Use of LiDAR among State Highway Agencies

LiDAR data is a promising and effective strategy for mapping detailed road infrastructure and conducting inundation analysis (Chen 2019). The research team reviewed how state highway agencies use LiDAR data and technologies for asset management. The review was based on the publications associated with each state Department of Transportation (DOT) and information available on their websites. The review found that most state DOTs (47 out of 50 state DOTs) use LiDAR for various purposes.

State DOTs have used LiDAR technologies for condition assessments of and data collection on various transportation infrastructures, such as pavement markings, traffic signals/signs, guardrails, retaining walls, bridges, and culverts. They have also used LiDAR for traffic pattern and speed monitoring and for environmental and geotechnical assessment such as slope

stability, geologic mapping, highway mapping and design, deformation monitoring on the landscape, geohazard mapping for landslides and floods, monitoring sea level in different salt marsh habitats for eco-habitats, analyzing archaeological sites, obtaining vegetation metrics, coastal zone erosion analysis, and monitoring volcanic activity. Twelve state DOTs (Alabama, Colorado, Idaho, Iowa, Kansas, Kentucky, North Carolina, North Dakota, Ohio, Pennsylvania, Tennessee, and Virginia) have used LiDAR for asset management by taking field surveys using LiDAR technologies and monitoring asset conditions. However, the project found no information about the use of LiDAR data for small water crossing asset management among state DOTs.

Chapter 2. Survey Study on Water Crossing Assets

2.1 Water Crossing Asset Data Development

This project aimed to develop an automated flood risk assessment system for small water crossings less than 20 feet in span on Missouri's highways that are not listed in the 2023 NBI. Thus, the project needed to identify the locations of those water crossings. Since there is no readily available inventory data for those structures, the project developed a process to identify the locations using the following steps.

First, the intersections of Missouri highways and waterways, using the 2019 Water Quality Standard (WQS) data from the Missouri Department of Natural Resources (MDNR) (MDNR, n.d.), were recorded and collected using GIS. The WQS data includes the locations of Missouri streams, which are required to be monitored for state water quality standards. The intersections potentially indicate the locations of water crossings such as bridges, culverts, or low water crossings (LWCs).

Second, water crossings not overlapped with bridges and culverts in the 2023 NBI data were identified. Figure 2.1, below, shows 10,060 water crossings on Missouri highways included in the NBI data. These NBI asset locations and the intersections between Missouri highways and the 2019 WQS data were spatially matched to identify potential non-NBI water crossings. Since the xy coordinates of the NBI assets were not geocoded at the centers of the assets, the project created a 300-foot buffer from all NBI assets.

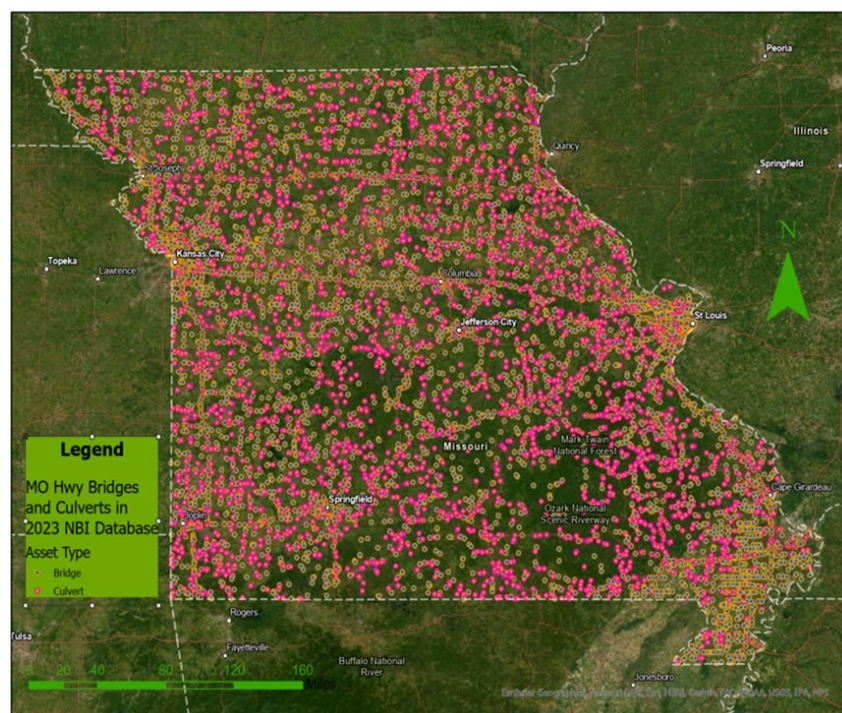


Figure 2-1. Bridge and Culvert Locations of the 2023 National Bridge Inventory (NBI) Data

Since there were numerous potential non-NBI assets in the state, the project team focused on accessible assets in the Kansas City metro area. Figure 2.2 below illustrates potential locations of non-NBI assets within the five counties (Cass, Clay, Jackson, Platte, and Ray Counties) in the metro area that do not spatially overlap the 2023 NBI assets. The project identified 1,292 potential non-NBI asset locations on Missouri highways within the five counties, as shown in Figure 2.2.

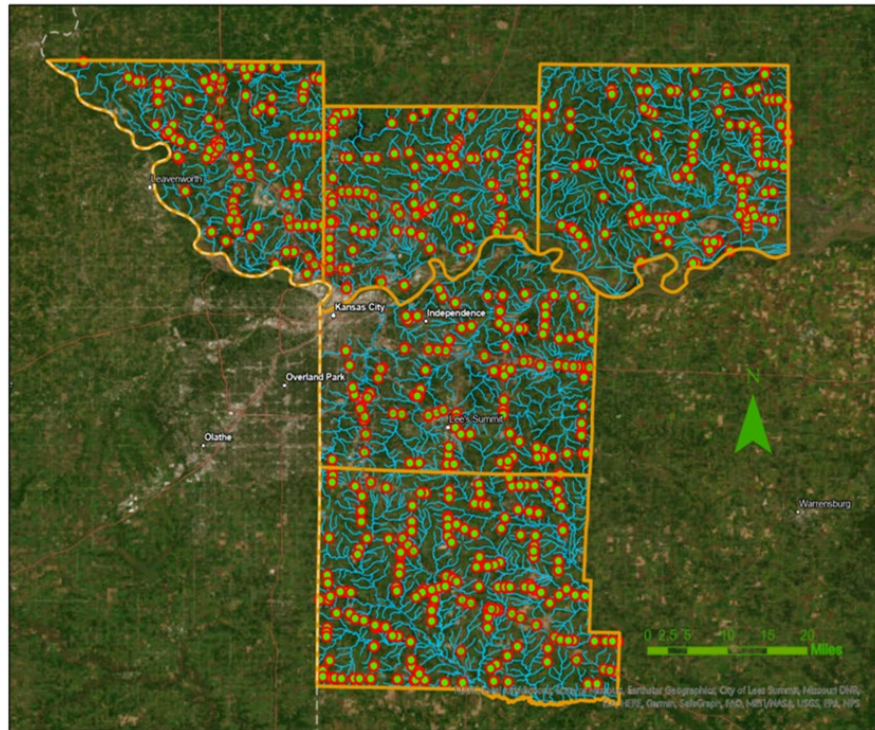


Figure 2-2. Potential Locations of Non-NBI Assets in the Kansas City Metro Counties

Third, non-NBI water crossing assets were identified for field data collection of asset characteristics. The project visually examined 1,292 potential non-NBI asset locations that do not overlap with NBI assets using Google Maps and Google Earth Pro, as shown in Figure 2.3 below. The project also searched for potential non-NBI water stream assets in Benton, Cedar, Dade, and Hickory Counties outside the Kansas City metro area.

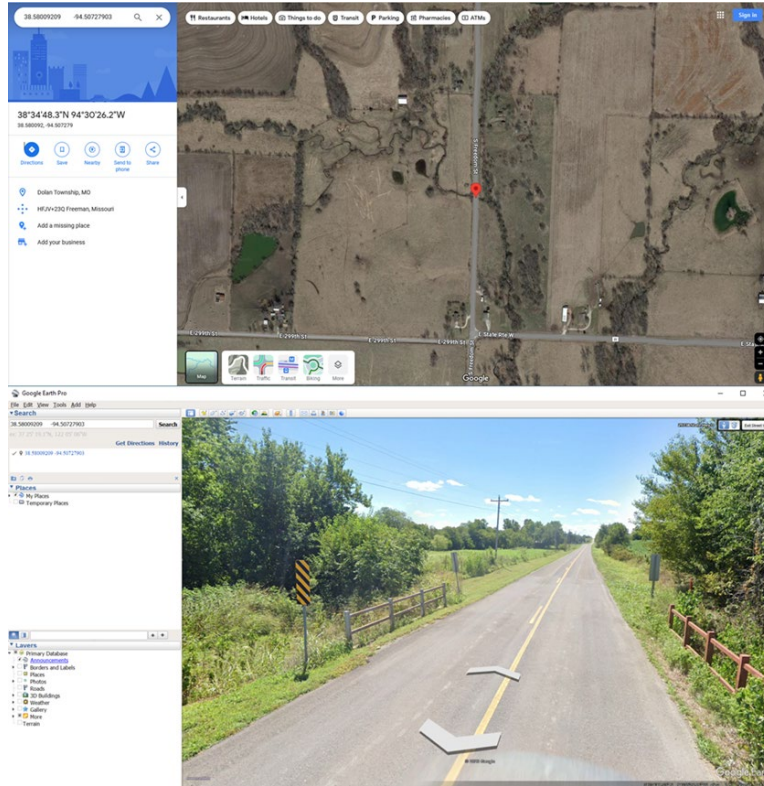


Figure 2-3. Water Crossing Site Screening using Google Maps and Google Earth

A number of potential non-NBI water crossing sites, particularly on minor streams, were found to have no water crossing assets. Through this process, a total of 125 sites were visited for asset measurements, as shown in Figure 2.4.



Figure 2-4. Surveying the Water Crossing Assets

However, during the site visits, a number of assets were unable to be surveyed due to access and safety issues (heavy vegetation, blocked logs, steep slopes, fences, animal presence such as snakes, contaminated water, high-speed traffic, structural safety, no available safe parking spots, etc.) as illustrated in Figure 2.5. As a result, the project successfully surveyed 53 water crossing assets. Ten sites were visited multiple times for remeasurement. Figure 2.6 shows the visited and measured non-NBI asset locations visited in the Kansas City metro area.



Figure 2-5. Examples of Unsurveyable Non-NBI Water Crossing Sites

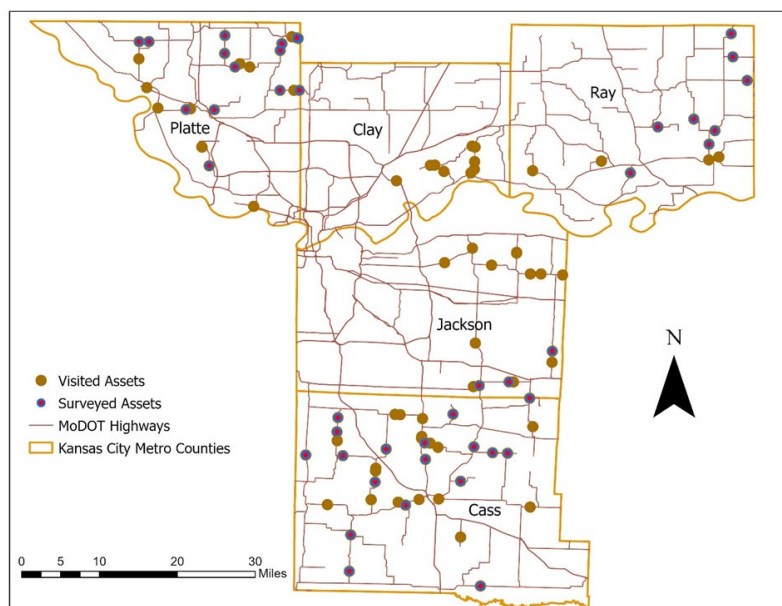


Figure 2-6. Visited and Surveyed Water Crossing Assets in the Kansas City Metro Counties

2.2 Surveyed Small Water Crossing Assets

Table 2-1 is a summary table of surveyed water crossing assets including 3 bridges, 36 culverts, and 14 LWCs. The project utilized tape measures and a non-proprietary LiDAR scanning program, Scaniverse (Scaniverse, n.d.), that can be installed on iPhone to take measurements. The project classified the non-NBI assets into three asset types: bridges, culverts, and LWCs. It should be noted that a structure spanning less than 20 feet is considered a culvert, not a bridge (FHWA 1995). Culverts are typically distinguished from bridges with covered embankments and have structural materials around the entire perimeter (FHWA 1995). For the purpose of the study, however, a culvert with an open bottom was classified as a bridge. An LWC was defined as a water crossing structure with an open area with the road surface that allows vehicles to cross a waterway when water levels are low but flooded during high water periods.

Table 2-1. Characteristics of Water Crossing Assets

Asset Type	Latitude	Longitude	Rise	Span	Diameter	Length	Embankment	County
Bridge	38.58009	-94.50728	5'	18' 1"	N/A	27'	15"	Cass
Bridge	38.75069	-94.37006	7' 8"	12' 2"	N/A	21' 8"	27"	Cass
Bridge	37.70233	-93.83248	67"	8'	N/A	31'	-	Cedar
Culvert, Single-barrel box	38.73924	-94.44150	7' 5"	14'	N/A	30'	N/A	Cass
Culvert, Single-barrel box	38.63533	-94.40570	7' 6"	10'	N/A	26' 3"	24"	Cass
Culvert, Single-barrel box	38.48509	-94.26626	6'	10'	N/A	29'	20"	Cass
Culvert, Single-barrel box	38.73224	-94.24416	8'	10'	N/A	29'	24"	Cass
Culvert, Single-barrel box	38.86382	-94.21365	8'	10'	N/A	40'	N/A	Jackson
Culvert, Single-barrel box	38.83355	-94.17536	4' 10"	7' 7"	N/A	28' 5"	18"	Cass
Culvert, Single-barrel box	38.92066	-94.13313	6'	8'	N/A	68'	N/A	Jackson
Culvert, single-barrel pipe	38.80406	-94.31766	N/A	N/A	56"	45' 3"	N/A	Cass
Culvert, double-barrel box	39.25183	-93.98801	8' 6"	8' 6"	N/A	23' 5"	20"	Ray
Culvert, Single-barrel box	39.33045	-93.83123	7' 7"	12'	N/A	32'	29"	Ray
Culvert, Single-barrel box	39.35183	-93.87057	7' 6"	10' 2"	N/A	23' 1"	24"	Ray
Culvert, Single-barrel box	38.51232	-94.51013	6'	7'	N/A	36' 4"	23"	Cass
Culvert, Single-barrel box	39.33706	-93.93680	6'	5'	N/A	24'	22"	Ray
Culvert, Single-barrel box	39.42310	-93.77132	7' 1"	13'	N/A	37' 4"	25"	Ray
Culvert, Double-barrel box	39.46718	-93.79789	8' 6"	12' 1"	N/A	26'	24"	Ray
Culvert, Single-barrel box	39.51020	-93.80078	8'	14' 6"	N/A	39' 3"	25"	Ray
Culvert, Single-barrel box	38.77127	-94.53298	5'	7'	N/A	37' 6"	17"	Cass
Culvert, Single-barrel box	38.72682	-94.52206	10'	14'	N/A	27'	27"	Cass
Culvert, Single-barrel box	38.72015	-94.36889	6'	8'	N/A	43'	25"	Cass
Culvert, double-barrel box	38.73140	-94.21640	6' 6"	8'	N/A	30' 6"	24"	Cass
Culvert, Single-barrel box	39.26487	-94.77028	7'	6'	N/A	38'	24"	Platte
Culvert, Single-barrel box	39.36921	-94.76081	5'	8'	N/A	39' 6"	19"	Platte
Culvert, Single-barrel box	39.36948	-94.81323	6'	8'	N/A	70'	26"	Platte
Culvert, Single-barrel box	39.49546	-94.90055	12'	12'	N/A	48'	32"	Platte
Culvert, Single-barrel box	39.50690	-94.74128	62"	7' 4"	N/A	37'	20"	Platte
Culvert, Double-barrel box	39.50151	-94.60510	8'	8'	N/A	32'	24"	Platte
Culvert, Single-barrel box	39.49157	-94.63514	7'	13'	N/A	40' 8"	27"	Platte
Culvert, Single-barrel pipe	39.47900	-94.63836	N/A	N/A	6'	40'	N/A	Platte
Culvert, Single-barrel box	39.47355	-94.74154	6' 7"	8' 2"	N/A	30'	36"	Platte
Culvert, Single-barrel box	39.44824	-94.72249	5'	5'	N/A	34' 7"	16"	Platte
Culvert, single-barrel pipe	39.40503	-94.63906	N/A	N/A	5'	47'	N/A	Platte
Culvert, Single-barrel box	39.40505	-94.60294	6'	10'	N/A	30' 6"	24"	Platte
Culvert, Single-barrel box	39.50222	-94.60748	7'	13'	N/A	30"	21"	Platte
Culvert, Single-barrel box	38.67932	-94.30344	6'	12'	N/A	28'	26"	Cass
Culvert, Single-barrel box	38.31468	-93.11042	5' 1"	12' 2"	N/A	28'	25"	Benton
Culvert, Single-barrel box	37.62439	-93.63216	6'	7'	N/A	33' 7"	-	Cedar
LWC, Single-barrel box	38.74354	-94.27875	4' 1"	12'	N/A	26'	41"	Cass
LWC, Double-barrel pipe	39.30491	-93.84213	4'	6' 3"	N/A	36' 1 "	13"	Ray
LWC, Double-barrel pipe	39.30491	-93.84213	4'	6' 3"	N/A	36' 1 "	13"	Ray
LWC, Single-barrel box	38.79775	-94.53133	3' 10"	6'	N/A	37' 6"	16.5"	Cass
LWC, Double-barrel box	38.31574	-93.10522	3' 2"	18' 2"	N/A	27' 7"	14"	Benton
LWC, Single-barrel box	38.67822	-94.46227	3' 7"	6'	N/A	25' 9"	N/A	Cass
LWC, Triple-barrel box	38.31510	-93.09910	2' 7"	97"	N/A	25' 5"	13"	Benton
LWC, Single barrel pipe	38.34109	-93.15506	N/A	N/A	4' 4"	40' 4"	N/A	Benton
LWC, Single-barrel box	37.72905	-93.90455	1' 8"	2'	N/A	26'	-	Cedar
LWC, Single-barrel box	37.72902	-93.88872	3'	64"	N/A	27'	-	Cedar
LWC, Single-barrel pipe	37.59040	-94.01094	N/A	N/A	4'	43'	-	Cedar
LWC, Double-barrel box	38.72849	-94.59071	3' 3"	12' 4"	N/A	32'	N/A	Cass
LWC, Triple-barrel box	38.02327	-93.14470	4'	6'	N/A	34'	N/A	Hickory
LWC, Single-barrel box	38.85680	-94.26883	6'	6'	N/A	44'	N/A	Jackson

Chapter 3. Hydraulic Model Development for Flood Risk Assessment

As the most common means of passing water from one side of a roadway to another (Greer, 2018), roadway culverts form a critical part of transportation infrastructure. Nevertheless, they are arguably the most neglected element in the system, according to the Federal Highway Administration (FHWA, 2014). While state transportation departments typically use sophisticated and dedicated management systems to track the condition and prioritize improvements for roads and bridges, culverts often remain unmarked, unknown, and neglected. State departments such as the Missouri Department of Transportation typically rely on maintenance workers to spot and report problems with existing culverts, according to FHWA (2014).

Automated and computer-aided monitoring and mapping technology could help inventory culverts and improve the effectiveness and efficiency of early-warning culvert maintenance programs. This could increase culvert life expectancy, reduce staff demands, and reduce the cost of planning, maintaining, and improving culverts. One such promising technology is GIS-enabled culvert monitoring. This project team developed an automated GIS workflow that can be used to identify, categorize, and analyze culvert assets remotely using widely available GIS data. It predicts locations where a culvert should exist based on topographic geometry and hydrology, estimates the culvert's likely dimensions, and predicts whether a culvert in the identified location would or would not overtop during different statistical storm events.

3.1 Model Workflow Overview

The automated culvert analysis workflow consists of a GIS analysis procedure in the QGIS desktop GIS application, which steps a user through a defined workflow of analysis evaluations to arrive at likely culvert location, geometry, hydrology, and overtopping attributes. QGIS is a cross-platform, open-source GIS, licensed under the GNU General Public License. It runs on Linux, Unix, Mac OSX, Windows, and Android, and supports numerous vector, raster, and database formats and functionalities. QGIS provides a continuously growing number of capabilities provided by core functions and plugins, permitting users to visualize, manage, edit, and analyze data, and compose printable maps. The QGIS model designer interface, Python programming language, and the PyQGIS python application programming interface were used to automate the analysis workflow for this project where practical.

3.1.1 Process Outline

The analysis workflow is a four-step process, as illustrated in Figure 3.1:

- Step 1 – Hydroconditioning of terrain data and stream delineation
- Step 2 – Culvert location and elevation data
- Step 3 – Culvert hydrology
- Step 4 – Culvert width and hydraulics

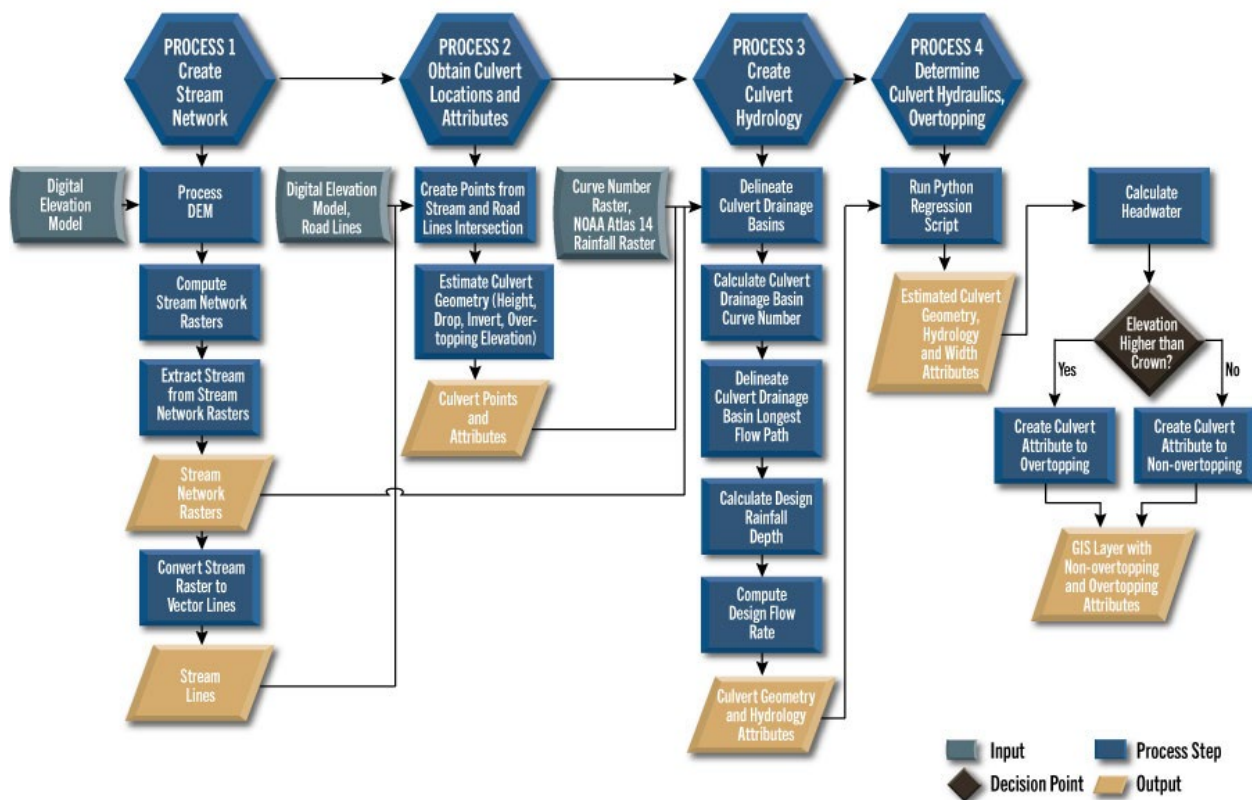


Figure 3-1. Process Flow Chart

3.1.2 Process Description

In this section, each process for the GIS evaluation will be described in further detail.

Process 1: Hydroconditioning and Stream Creation

The first process uses any existing bare-earth digital elevation model (DEM) map that contains culvert or likely culvert locations. The DEM is first "hydroconditioned," and then the streams are delineated. Hydroconditioning of a DEM is a process necessary to modify the digital topography in such a way that runoff flow directions can be algorithmically determined. In effect, hydroconditioning removes or creates passages through barriers in the terrain that might trap or impede water flow, such as deep depressions, dams, and elevated roadbeds, allowing water in the model to drain from any point on the topography without getting trapped. This process requires that pits and depressions in the DEM be breached or filled. In this way, algorithms can determine the flow path that surface runoff would likely follow from any point in the raster DEM, more accurately simulating how hydrology for a watershed would behave in the real world.

To ensure that the potential locations of culverts in the terrain are located as accurately as possible, the method of hydroconditioning known as "breaching" is used. Breaching punches a hole or breaks through a barrier to flow, such as a dam or low area, permitting the simulated water flow to exit any area in which it might otherwise be trapped. Prioritizing breaching, as opposed to other common hydroconditioning methods such as filling sinks, burning streams, and building wall ridges, results in a smaller percentage of cells in the DEM being modified and ensures the simulated flow crosses embankments at a location more likely to be relatively close to a true culvert location. After the DEM is hydroconditioned, a D8 flow direction raster and a D8 flow accumulation raster are produced; these rasters are used to produce a vector stream layer. D8 flow direction is the direction of the steepest downward slope on the eight surrounding grids of a 3x3 block centered grid.

Process 2: Culvert Locations and Elevation Attributes

The second process overlays the input DEM raster with a line vector of a known road along with the stream line vector layer created in the previous process. Using the intersection of those two inputs, it predicts likely culvert locations. It also assigns elevation attributes to the culvert layer based on the elevation value sampled from the input DEM. To reduce computing demands and eliminate the need to check if each resulting culvert is under MoDOT maintenance, the input roads layer should only include roads that the user is interested in. MoDOT or the U.S. Census Bureau's TIGER/Line Roads files can be used and filtered by road type and jurisdiction to limit the number of analyzed roadways.

Process 3: Culvert Hydrology

In Process 3, the culvert point locations from Process 2 and the hydroconditioned DEMs from Process 1 are used to determine and map the subbasin area that drains to each identified culvert. It then computes the necessary hydrologic input parameters for the subbasin to be input into a hydrologic model to estimate the amount of surface runoff expected to reach that culvert location from any given rainfall event. The hydrologic model uses the U.S. Department of Agriculture's Soil Conservation Service curve number method to account for factors that may affect runoff, including soil type, existing soil moisture at the start of the storm, and land use and vegetation in the subbasin. The hydrologic model uses a statewide curve number raster, representing a specific land cover in combination with soil type. For precipitation input, it uses a precipitation frequency estimate from the NOAA Atlas 14 precipitation frequency data server provided by the US Department of Commerce's National Oceanic and Atmospheric Administration. Process 3 ultimately computes the peak design storm discharge. Process 3 also optionally outputs delineated subbasin polygons and longest flow paths.

Process 4: Culvert Hydraulics

Using the attribute values assigned to each potential culvert location point in Processes 2 and 3, Process 4 performs culvert hydraulic computations for each identified culvert location in the culvert layer. It then compares the computed water surface elevation against the estimated crown of the road elevation and determines whether the culvert will overtop for a particular design storm.

3.2 Hydrology

To determine if a given culvert is likely to overtop, a design flow rate must first be defined. Design flow rates are generally defined by the recurrence interval of the storm—that is, the statistical likelihood that a storm of that magnitude will occur in any given year—that will produce the flow rate. Design flow rates also depend on the amount of water from a storm event that does not soak into the ground and, therefore, runs off. That runoff can be estimated using hydrologic parameters. A hydrologic parameter is a variable that describes and quantifies the characteristics of a watershed that influences the behavior of rainfall and runoff within the watershed. The parameters are input into hydrologic models to predict the amount of runoff a given amount of rainfall can be expected to produce.

3.2.1 Methodology

The Natural Resources Conservation Service (NRCS) Curve Number method was selected for use with the plugin developed for this project. The NRCS curve number method runoff equation is (Mockus and Moody 2004):

$$Q = (P - I_a)^2 / (P - I_a + S)$$

where:

Q is the direct runoff depth,

P is the event rainfall depth,

S is the site storage index, defined as the maximum possible difference between P and Q as $P \rightarrow \infty$,

$P - I_a$ is also called "effective rainfall" or P_e (Hawkins, 2002),

CN is related to S by the equation $CN = 1000 / (10 + S)$,

I_a is an "initial abstraction," or event rainfall required to initiate runoff.

Equation 3-1. Direct Runoff Depth for $P \geq I_a$ ($Q=0$ if $P < I_a$)

The initial abstractions are computed with the following equation:

$$I_a = \lambda S$$

where:

I_a is the Initial abstraction,

λ is the initial abstraction ratio, with a default value of 0.2.

Equation 3-2. Initial Abstractions

The estimation of hydrology parameters was computed using existing QGIS processing algorithms. A statewide curve number raster was created using soil data from the U.S. Department of Agriculture's Soil Survey Geographic Database and land use patterns from the USGS's National Land Cover Database (NLCD) (Dewitz, 2023).

3.2.2 Parameter Estimation

Parameters developed include the following:

- Basin area
- Longest flow path
- Basin slope
- Curve number
- Time of concentration

Basin area, longest flow path, and basin slope were calculated using existing tools contained within the WhiteboxTools QGIS plugin. The curve number is weighted from a curve number raster created using National Land Cover Database (NLCD) landcover data and Soil Survey Geographic Database (SSURGO) soil data with statewide coverage. The time of concentration is estimated from these calculated parameters using the NRCS watershed lag method, as described in National Engineering Handbook (NEH) 630.1502, using the following equation:

$$T_c = l^{0.8} \frac{(S + l)^{0.7}}{1140Y^{0.5}}$$

where:

- T_c is the time of concentration in hours,
- l is the flow length in feet,
- Y is the average watershed land slope in percent,
- S is the maximum potential retention in inches.

Equation 3-3. Time of Concentration

3.3 Width Regression

Once the expected flow to the identified culvert is estimated through the hydrologic calculations, it is time to estimate its propensity to overtop during a specific storm event. Determining this requires knowing the volume of flow the culvert can pass based on its dimensions.

3.3.1 Methodology

Remotely estimating the width of a culvert using its elevation and computerized interpretation of satellite imagery is possible, in theory. However, it is an extremely difficult task, requiring an impractical amount of data necessary to train the algorithm. Alternatively, estimating a culvert's width using basin hydrological parameters via regression is a comparatively simple task, once the basin hydrological parameters are determined from existing readily available GIS data.

It was hypothesized that the following variables likely correlate to culvert sizing:

- Basin area
- Basin or flow path slope
- Longest flow path length
- Curve number

- Time of concentration
- Valley side slope

3.3.2 Correlation Results

A correlation matrix was computed to better determine the variables most associated with culvert sizing, as shown in Table 3-1. The data used for the correlation was based on the information collected from the asset survey described previously in this report. The open-source Python library scikit-learn, a machine learning predictive data analysis library for Python that includes tools for regression and model selection, was used.

Table 3-1. Correlation Matrix

	Height	Width	Flowpath slope	Length	Basin area	CN	Tc	Valley side slope
Height	1.0000	0.4025	-0.6427	0.7283	0.8300	-0.1726	0.7757	0.0656
Width	0.4025	1.0000	-0.4343	0.4287	0.4938	-0.3995	0.5438	-0.2945
Flowpath slope	-0.6427	-0.4343	1.0000	-0.4968	-0.5310	0.2424	-0.7049	-0.0848
Length	0.7283	0.4287	-0.4968	1.0000	0.9199	-0.0890	0.9119	0.1682
Basin area	0.8300	0.4938	-0.5310	0.9199	1.0000	-0.1604	0.8764	0.0934
CN	-0.1726	-0.3995	0.2424	-0.0890	-0.1604	1.0000	-0.3945	0.1688
Tc	0.7757	0.5438	-0.7049	0.9119	0.8764	-0.3945	1.0000	0.0594
Valley side slope	0.0656	-0.2945	-0.0848	0.1682	0.0934	0.1688	0.0594	1.0000

Table 3-1 illustrates the correlation between the culvert geometry variables and the culvert hydrologic variables. Each cell in the matrix is given a value between negative one and one. A negative one represents the strongest possible negative correlation, meaning as the value in the x variable increases the value of the y variable decreases. A positive one represents the strongest possible positive correlation, meaning as the value of the x variable increases the value of the y variable increases. Values closer to zero indicate that the two variables do not correlate to one another. For the purposes of predicting culvert width from hydrologic variables, a strong negative correlation is equally useful as a strong positive correlation.

Based on the correlation analysis, basin area, flow path length, and basin time of concentration were the strongest predictors of culvert width. Since time of concentration is primarily a function of basin area and flow length, the final regression equation predicted culvert width as a function of basin area and flow length only.

3.4 Culvert Hydraulics

The culvert hydraulics were analyzed using established FHWA procedures described in the following sections.

3.4.1 Methodology

Once the predicted dimensions of the identified culvert structure are calculated from the hydrologic study, further analysis of the predicted depth of flow to be expected through the culvert is conducted. Hydraulic calculations use Python scripting based on the FHWA's comprehensive culvert design guidance document, Hydraulic Design Series Number 5 (HDS 5) (Schall et al. 2012). The scripted computations check both inlet and outlet control conditions and estimate the water surface elevation directly upstream of the culvert using the more conservative control condition.

The following equations are used for inlet control in this study:

$$\frac{HW_i}{D} = \frac{H_c}{D} + K \left[\frac{K_u Q}{AD^{0.5}} \right]^M + K_s S$$

where:

HW_i is the headwater depth above inlet control section invert in feet

D is the interior height of culvert barrel in feet,

H_c is the specific head at critical depth ($d_c + V_c^2/2g$) in feet,

Q is the discharge, in cubic feet per second,

A is the full cross-sectional area of culvert barrel in square feet,

S is the culvert barrel slope in feet per foot,

K, M, Y are the constants from Tables A.1, A.2, A.3 from HDS5 Appendix A,

K_u is the unit conversion 1.0 (1.811 SI),

K_s is the slope correction, -0.5 (mitered inlets +0.7).

Equation 3-4. Unsubmerged Inlet Control

$$\frac{HW_i}{D} = c \left[\frac{K_u Q}{AD^{0.5}} \right]^M + y + K_s S A$$

where:

HW_i is the headwater depth above inlet control section invert, in feet,

D is the interior height of culvert barrel, in feet,

H_c is the specific head at critical depth ($d_c + V_c^2/2g$), in feet,

Q is the discharge, in cubic feet per second,

A is the full cross sectional area of culvert barrel, in square feet,

S is the culvert barrel slope, in feet per foot,

K, M, c , and y are the constants from Tables A.1, A.2, A.3 from HDS5 Appendix A,

K_u is the unit conversion 1.0 (1.811 SI)

K_s is the slope correction, -0.5 (mitered inlets +0.7)

Equation 3-5. Submerged Inlet Control

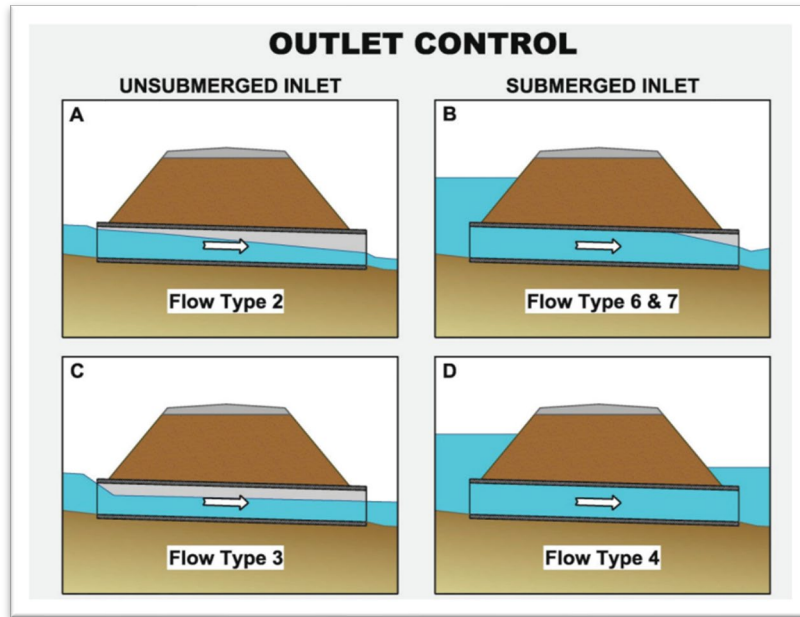


Figure 3-2. HDS 5 Outlet Control Flow Types

For outlet control, full flow in the culvert barrel is assumed, as shown in Figure 3.2 Picture D, as taken from HDS 5.

This study recognizes that not every variable that influences culvert hydraulics can be inferred from available GIS data in an automated manner, including such variables as the shape of the culvert and the conditions at the culvert entrance. To allow automated calculations, the following simplifying assumptions were made:

- Constant culvert length of 30 feet
- Constant slope value of 2 percent (0.02)
- Constants K, M, c, and Y assumed values for rectangular box concrete 0° wingwall flares, based on Chart 8, Scale 3 Equation form 1 from HDS-5 Table A.1.

3.4.2 Parameter estimation

For hydraulic calculations, the estimated culvert height is computed from the elevation DEM raster. The cover depth between the crown of the road and the top of the culvert is assumed to be a constant six inches. The calculated height is constrained to a minimum of three feet. A buffer distance is applied to the DEM from the culvert point. The crown height is assumed to be the maximum DEM elevation within this buffer distance. The invert height is assumed to be the minimum DEM elevation within this buffer distance. To estimate the width of the culvert, the regression equation relating culvert width to hydrologic parameters, as explained in 3.3 Width Regression on page 18 of this report, was used.

3.5 Plugin development

A QGIS Python plugin was developed for ease of installation and use. The QGIS python application programming interface PyQGIS was utilized for this task. The developed QGIS plugin can be added to

a user's QGIS installation via a ZIP file. The plugin also includes default curve number, terrain DEM, and rainfall point depth raster datasets. Installation and use instructions are included in the appendix to this report.

3.6 Assessment of Hydraulic Model Results

Hydraulic result validation is presented below. Hydrology results were not validated as they use long established industry standard methods. A HEC-RAS 2D model was developed to validate plugin hydraulic results. The 2D model utilized the same DEM elevation data as the plugin, however the culvert geometry data was taken from field measurements. The goal of validating the plugin against the 2D HEC-RAS model was to show that the plugin arrives at similar results to established culvert modeling methodologies. The HEC-RAS 2D modeling models the surface flow using the 2D shallow water equations, and the culverts are represented using a built-in sub routine, which calculates the flow through the culvert using the same FHWA culvert equations used in the plugin. An example of the HEC-RAS culvert section is shown in Figure 3.3. HEC-RAS and plugin modeling results are shown in Table 2-2.

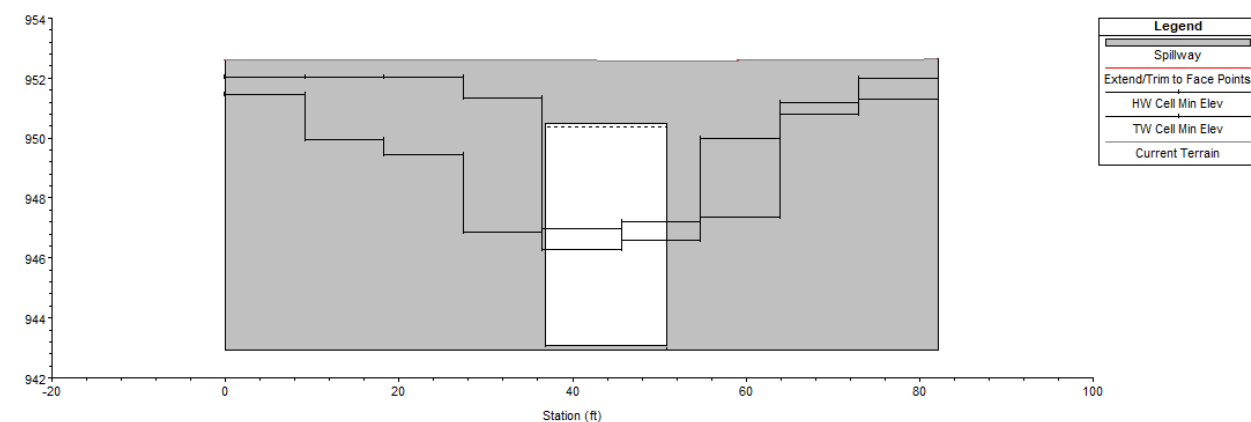


Figure 3-3. Example of HEC-RAS Cross-Section Showing the Culvert Opening

The results in Table 2-2 demonstrate the feasibility of using this tool to more efficiently identify undersized water crossings. Only one out of the 22 assets used in the validation of the MoACAT tool was not identified as a culvert crossing by MoACAT. Out of the four assets that were found to be overtopping using HEC-RAS, two were identified as overtopping by the MoACAT tool. It is worth noting that one of the assets identified as overtopping by HEC-RAS but not by MoACAT, was only marginally overtopping in the HEC-RAS model with a depth of 0.06 feet and a flow rate of 3.66 CFS. There was only one asset that MoACAT incorrectly identified as overtopping compared to the HEC-RAS results.

Table 3-2. GIS Plugin Validation Results

Asset	HH HEC- RAS	HH MoACAT	MoACAT Overtop	HEC- RAS Overtop	Qp	No of Barrels (Survey)	Height		Width	
							MoACAT	Survey	MoACAT	Survey
30	5.25	5.84	no	no	361.1	1	8.81	7	11.65	12
24	4.98	12.01	yes	yes	546.7	1	4.64	4	8.47	6
64	6.58	6.36	no	no	365.1	1	9.64	6	10.75	8
14	6.44	7.48	no	no	579.5	1	11.49	12	14.36	14
28	3.96	3.67	no	no	115.9	1	5.95	3.58	7.2	6
79	6.11	6.32	no	no	444.6	1	9	6	12.09	12
11	5.36	4.62	no	no	244	1	6.39	5	9.43	7
15	4.47	4.54	no	no	269.9	2	5.83	3.25	10.17	11.5
12	6.52	6.98	no	no	573.2	1	9.4	7.42	12.78	14
438	9.48	8.71	no	no	968.7	1	8.63	8.5	14.41	12
542	8.69	17.4	yes	yes	788.8	1	3	8	14	8
532	7.33	6.16	no	no	243.6	1	9.43	6	7.7	5
1189	7.57	6.43	no	no	531.9	1	5.67	7.5	12.4	10.16
1157	6.42	7.82	no	no	479.6	1	12.42	7.5	11.85	12
512	6.32	7.75	yes	no	507.4	1	3.63	7	12.9	13
1139	-	-	-	-	-	-	-	-	-	-
204	6.92	7.5	no	no	267.9	1	13.14	7	10.35	6
E1	2.3	3.07	no	no	188.9	2	3.2	9	11.5	22
168	4.74	5.16	no	no	202.3	1	8.28	5	8.54	8
332	4.75	4.8	no	no	151.6	1	7.62	6	6.76	8
200	5.86	6.2	no	yes	177.3	1	10.2	5	6.5	5
657	5.73	6.85	no	no	274.9	1	11.5	7.5	9.8	8.17
655	6.99	3.83	no	no	133.8	1	12.49	5.17	6.12	7.33
741	6.7	11.35	no	no	515.8	1	12	12	11.95	12

The RMSE (Root Mean Squared Error) for the difference in water depth between the HEC-RAS results and the MoACAT results was 1.05 feet. For culvert height, the RMSE for the difference between the surveyed height and model-predicted height was 3.7 feet. For the width, the RMSE for the difference in surveyed width and model-predicted width was 3.13 feet. These results are comparable to what is typically used to determine culvert geometry from planning level dam breach analyses. For these planning level dam breach analyses the culvert geometry is routinely manually estimated from available LiDAR data and aerial imagery.

Chapter 4. Conclusions and Recommendations

More frequent and larger flood events pose significant challenges to highway agencies in maintaining highway assets, particularly water crossing assets. Information on small water crossing assets is often limited and not readily available, making it difficult to assess the flood risks of those assets. Increasingly available high-resolution LiDAR data can facilitate identifying the locations and flood risks of the assets. This study developed a flood risk assessment tool for culverts, the most common type of small water crossings.

The MoACAT tool was developed with the goal of estimating culvert geometry by automating the process commonly utilized during planning-level dam breach analyses. For tool development, asset geometry information was collected via field surveys. The MoACAT tool was then developed to automate the necessary hydrology and hydraulic analyses needed to determine a culvert crossing's hydraulic capacity using readily available LiDAR DEM data.

The GIS algorithms utilized to determine culvert height automate this process, pulling directly from the LiDAR elevation data, in a similar manner to the manual process of looking at the channel invert elevation and the road crown elevation and assuming a depth of cover. The manual process used to determine culvert width and opening utilizes aerial imagery, so long as it is not obscured by trees or other obstructions. Directly automating this process through AI or other methods proved impractical, so a regression analysis of culvert basin hydrology was utilized instead. Established GIS methods for determination of hydrological parameters were utilized for both inputs into the width regression and inputs into the hydrology model used to determine an analysis event flow rate. Then, the culvert hydraulic capacity was analyzed using a Python script that utilized the FHWA HDS-5 methodology. GIS software, QGIS, and its Python api pyQGIS were utilized to present the tool in a user-friendly GUI environment as a QGIS plugin. The use of non-proprietary open-source QGIS can make the MoACAT tool more accessible and broadly applicable.

The hydraulic model results demonstrate the feasibility of this tool in effectively and efficiently assessing if water overtopping is occurring and identifying undersized water crossings. There was only one asset that MoACAT incorrectly identified as overtopping when compared to the HEC-RAS results. For culvert height and width, the RMSE for the difference between the surveyed and model-predicted height was comparable to what is typically used to determine culvert geometry from planning level dam breach analyses.

The MoACAT tool has significant potential to facilitate MoDOT in identifying and managing small flood-prone water crossing assets. This information can be used for highway and emergency management, prioritizing highway infrastructure investment to safeguard water crossing infrastructure and road users, providing efficient, reliable, and safe transportation networks, and ensuring efficient water crossing asset management. The MoACAT tool could be rolled into a future statewide flood prediction system for planning purposes. Culverts identified as likely to overtop by this tool should be verified through field data collection and more detailed analysis. The plugin's most significant strength is its ability to quickly identify assets that should be investigated in further detail to determine overtopping risk.

There are some limitations. The MoACAT tool is currently limited to box culverts. Box culverts are the most typical small water crossing asset. Most small assets we observed during the project were box culverts. A limited number of other water crossing assets (pipe culverts and LWCs) were challenging for hydraulic modeling, and small bridges may not significantly differ from box culverts. HEC-RAS can model LWCs. However, it is usually done by modeling them as culverts. The roadway profile is just lower. The regression width methodology is unlikely to accurately predict culvert open width in the case of culverts that were undersized due to errors in hydrology calculations. Lastly, the tool cannot account for culverts with very steep slopes and deep cover between the crown of the road and the top of the culvert.

In its current state, it is recommended that the MoACAT tool be used by an engineer or GIS technician with a strong knowledge of spatial analysis and basic Python scripting skills. It is recommended that the tool be used for an area no larger than one county at a time. Once culverts have been identified as overtopping, field data should be collected on the overtopping, and a traditional hydrologic analysis should be performed to confirm the results.

The recommended next steps are to improve the user interface and investigate methods that can identify culverts with extreme slopes or deep cover. It is also recommended that further development of the AI algorithm used to determine culvert geometry from field LiDAR data is conducted so that it can be utilized in the collection of field data for more detailed analysis of assets that the MoACAT plugin identified as overtopping.

References

- Adger, W. N. 2006. "Vulnerability." *Global Environmental Change*, 16(3): 268–281. Accessed December 26, 2024. <https://doi.org/10.1016/j.gloenvcha.2006.02.006>.
- Ai, C., and Tsai, Y. J. 2016. "An Automated Sign Retroreflectivity Condition Evaluation Methodology Using Mobile LiDAR and Computer Vision." *Transportation Research Part C: Emerging Technologies*, 63: 96–113. Accessed December 26, 2024. <https://doi.org/10.1016/j.trc.2015.12.002>.
- Amatya, D., Trettin, C., Panda, S., and Ssegane, H. 2013. "Application of LIDAR Data for Hydrologic Assessments of Low-Gradient Coastal Watershed Drainage Characteristics." *Journal of Geographic Information System*, 5(2): 175-191. Accessed December 26, 2024. <https://doi.org/10.4236/jgis.2013.52017>.
- Barclay, N., and M. Smith. (2021). "Assessment of Advanced LIDAR based Tools for Enhanced Flood Prediction." *SoutheastCon 2021*, ii 2, 1-5. Atlanta, GA. Accessed December 26, 2024. <https://doi.org/10.1109/southeastcon45413.2021.9401895>.
- Blöschl, G., Buttinger-Kreuzhuber, A., Cornel, D., Eisl, J., Hofer, M., Hollaus, M., Horváth, Z., Komma, J., Konev, A., Parajka, J., Pfeifer, N., Reithofer, A., Salinas, J., Valent, P., Vyleta, R., Waser, J., Wimmer, M. H., & Stiefelmeyer, H. 2024. "Hyper-Resolution Flood Hazard Mapping at the National Scale." *Natural Hazards and Earth System Sciences*, 24(6): 2071-2091. Accessed December 26, 2024. <https://doi.org/10.5194/nhess-24-2071-2024>.
- Bodoque, J. M., Aroca-Jiménez, E., Eguibar, M. Á., and J. A. García. 2022. "Developing Reliable Urban Flood Hazard Mapping from LiDAR Data." *Journal of Hydrology*, 617: 128975. Accessed December 26, 2024. <https://doi.org/10.1016/j.jhydrol.2022.128975>.
- Boumis, G., Moftakhari, H. R., and Moradkhani, H. 2023. "Coevolution of Extreme Sea Levels and Sea-Level Rise under Global Warming." *Earth's Future*, 11(7): e2023EF003649. Accessed December 26, 2024. <https://doi.org/10.1029/2023ef003649>.
- Brody, S. D., Blessing, R., Sebastian, A., and Bedient, P. 2012. "Delineating the Reality of Flood Risk and Loss in Southeast Texas." *Natural Hazards Review*, 14(2): 89–97. Accessed December 26, 2024. [https://doi.org/10.1061/\(asce\)nh.1527-6996.0000091](https://doi.org/10.1061/(asce)nh.1527-6996.0000091).
- Bruno, L. S., Mattos, T. S., Oliveira, P. T. S., Almagro, A., and Rodrigues, D. B. B. 2022. "Hydrological and Hydraulic Modeling Applied to Flash Flood Events in a Small Urban Stream." *Hydrology*, 9(12): 223. Accessed December 26, 2024. <https://doi.org/10.3390/hydrology9120223>.
- Chang, L., and Huang, S. 2015. "Assessing Urban Flooding Vulnerability with an Emergy Approach." *Landscape and Urban Planning*, 143: 11–24. Accessed December 26, 2024. <https://doi.org/10.1016/j.landurbplan.2015.06.004>.

- Chen, Q. 2019. *Ultra-high-accuracy Digital Terrain Model Mapping for Assessing Roadway Vulnerability to Sea-level Rise and Flooding: An Integrated Analysis of Mobile and Airborne LiDAR Data*. PSR-UH-18-41, Pacific Southwest Region UTC at the University of Hawaii. Accessed December 26, 2024. https://metrans.org/assets/research/psr-uh-18-41_chen_final-report.pdf.
- DHI. MIKE Software. Accessed December 26, 2024. <https://www.dhigroup.com/technologies/mikepoweredbydhi/mikeplus-2d-overland>.
- Dewitz, J. 2023. National Land Cover Database (NLCD) 2021 Products: U.S. Geological Survey data release. Multi-Resolution Land Characteristics Consortium. Accessed on December 26, 2024. <https://doi.org/10.5066/P9JZ7AO3>.
- Environmental Protection Agency (EPA). n.d. *Climate Change Indicators: River Flooding*. U.S. Department of the Interior. Accessed December 26, 2024. <https://www.epa.gov/climate-indicators/climate-change-indicators-river-flooding#ref4>.
- Federal Emergency Management Agency n.d. National Flood Hazard Layer. Accessed December 26, 2024. <https://www.fema.gov/flood-maps/national-flood-hazard-layer>.
- Federal Emergency Management Agency (FEMA). 2017. *Floodmap Glossary*. Accessed December 26, 2024. https://floodmaps.fema.gov/tutorials/check-ras/0.3_glossary.shtml.
- Federal Highway Administration (FHWA). n.d. *Download NBI ASCII files 2023*. Accessed December 26, 2024. <https://www.fhwa.dot.gov/bridge/nbi/ascii2023.cfm>.
- Federal Highway Administration (FHWA). 1995. *Recording and Coding Guide for the Structure Inventory and Appraisal of the Nation's Bridges*. U.S. Department of Transportation, Report No. FHWA-PD-96-001. Accessed December 26, 2024. <https://www.fhwa.dot.gov/bridge/mtguide.pdf>.
- Federal Highway Administration (FHWA). 2014. "Culvert management case studies: Vermont, Oregon, Ohio, and Los Angeles County." Accessed December 26, 2024. <https://www.fhwa.dot.gov/asset/pubs/hif14008.pdf>.
- Gallagher, J. 2014. "Learning about an Infrequent Event: Evidence from Flood Insurance Take-Up in the United States." *American Economic Journal Applied Economics*, 6(3): 206–233. Accessed December 26, 2024. <https://doi.org/10.1257/app.6.3.206>.
- Gargoum, S. A., Karsten, L., El-Basyouny, K., and Koch, J. C. 2018. "Automated Assessment of Vertical Clearance on Highways Scanned Using Mobile LiDAR Technology." *Automation in Construction*, 95: 260–274. Accessed December 26, 2024. <https://doi.org/10.1016/j.autcon.2018.08.015>.

- Gharaibeh, N. G., Lee, C.-C. (Barry), Alhalbouni, T., Wang, F., Lee, J., Newman, G., Güneralp, B., and Van Zandt, S. 2023. "Quality of Stormwater Infrastructure Systems in Vulnerable Communities: Three Case Studies from Texas." *Public Works Management Practices*, 28(4): 518–536. <https://doi.org/10.1177/1087724x231164415>.
- Guan, H., Li, J., Cao, S., and Yu, Y. 2016. "Use of Mobile LiDAR in Road Information Inventory: A Review." *International Journal of Image and Data Fusion*, 7(3): 219–242. Accessed December 26, 2024. <https://doi.org/10.1080/19479832.2016.1188860>.
- Hans, Z., S. Hallmark, R. Souleyrette, R. Tengens, and D. Veneziano. (2003). *Use of LIDAR-based Elevation Data for Highway Drainage Analysis: A Qualitative Assessment*. Midwest Transportation Consortium at the Center for Transportation Research and Education (CTRE) at Iowa State University. Accessed December 26, 2024. https://publications.iowa.gov/21032/1/IADOT_LIDAR_Based_Elevation_Data_Drainage_Analysis_Qualitative_Assessment_2003.pdf.
- Hou, Q., and Ai, C. 2020. "A Network-level Sidewalk Inventory Method Using Mobile LiDAR and Deep Learning." *Transportation Research Part C: Emerging Technologies*, 119: 102772. Accessed December 26, 2024. <https://doi.org/10.1016/j.trc.2020.102772>.
- Kolaković, S., Kolaković, S., Fabian, J., Jeftenić, G., and Trajković, S. 2021. "River Floodplain 1D/2D Hydraulic Modelling Combined with Recent LiDAR DTM Technology." *Tehnicki Vjesnik - Technical Gazette*, 28(3): 880-890. <https://doi.org/10.17559/tv-20200429024034>.
- Li, M., Li, X., Wu, D., Zou, L., and Huang, X. 2023. "Digitizing and Inventorying Traffic Control Infrastructures: A Review of Practices." *Transportation Research Interdisciplinary Perspectives*, 21: 100879. Accessed December 26, 2024. <https://doi.org/10.1016/j.trip.2023.100879>.
- Mallakpour, I., and Villarini, G. 2015. "The Changing Nature of Flooding Across the Central United States." *Nature Climate Change*, 5: 250–254. Accessed December 26, 2024. <https://doi.org/10.1038/nclimate2516>.
- Martin, M. A., Jahanger, Q. K., Zimmerman, G., Hadziomerspahic, A., Sillars, D. N., Ng, E. H., and Calvo-Amodio, J. 2020. "Case Study: Economic Analysis of Statewide Roadway 3D Mapping Using Mobile LIDAR." *Journal of Transportation Engineering, Part A: Systems*, 146(7): 05020004. Accessed December 26, 2024. <https://doi.org/10.1061/jtepbs.0000377>.
- Missouri Department of Natural Resources (MDNR). 2019 Water Quality Standard (WQS) data. Accessed December 26, 2024. <https://data-msdis.opendata.arcgis.com/datasets/MSDIS::mo-2019-wqs-stream-classifications-and-use/about>.
- Mockus, V. and Moody, H. F. 2004. *Part 630 Hydrology National Engineering Handbook, Chapter 9 Hydrologic Soil-Cover Complexes*. NRCS USDA eDirectives. Accessed on December 26, 2024. <https://directives.sc.egov.usda.gov/landingpage/79824ad0-6672-4e3b-b100-86d87993f172>.

- National Weather Service (NWS). n.d. *NWS Preliminary US Flood Fatality Statistics*. Accessed December 26, 2024. <https://www.weather.gov/arx/usflood>.
- Patterson, L. A., and Doyle, M. W. 2008. "Assessing Effectiveness of National Flood Policy through Spatiotemporal Monitoring of Socioeconomic Exposure. *JAWRA Journal of the American Water Resources Association*, 45(1): 237–252. Accessed December 26, 2024. <https://doi.org/10.1111/j.1752-1688.2008.00275.x>
- Pregolato, M., Ford, A., Wilkinson, S. M., and Dawson, R. J. 2017. "The Impact of Flooding on Road Transport: A Depth-disruption Function." *Transportation Research Part D: Transport and Environment*, 55: 67-81. Accessed December 26, 2024. <https://doi.org/10.1016/j.trd.2017.06.020>.
- Ramachandran, R., Fernández, Y. B., Truckell, I., Constantino, C., Casselden, R., Leinster, P., and Casado, M. R. 2023. "Accuracy Assessment of Surveying Strategies for the Characterization of Microtopographic Features That Influence Surface Water Flooding." *Remote Sensing*, 15(7): 1912. Accessed December 26, 2024. <https://doi.org/10.3390/rs15071912>.
- Sairam, N., Nagarajan, S., and Ornitz, S. 2016. "Development of Mobile Mapping System for 3D Road Asset Inventory." *Sensors*, 16(3): 367. Accessed December 26, 2024. <https://doi.org/10.3390/s16030367>.
- Scaniverse. n.d. <https://scaniverse.com/>. Accessed January 15, 2024.
- Schall, James D., Thompson, Philip L., Zerges, Steve M., Kilgore, Roger T., and Morris, Johnny L.. 2012. "HYDRAULIC DESIGN OF HIGHWAY CULVERTS Third Edition". US Department of Transportation, Federal Highway Administration.
- Strong, N., and Holt, M. 2011. "Automated Land Use and Vegetation Monitoring to Enable Efficient Management of Britain's Off Track Railway Assets." *5th IET Conference on Railway Condition Monitoring and Non-Destructive Testing (RCM 2011)*, 612. Accessed December 26, 2024. <https://doi.org/10.1049/cp.2011.0612>.
- Tabari, H. 2020. "Climate Change Impact on Flood and Extreme Precipitation Increases with Water Availability. *Scientific Reports*, 10: 13768. Accessed December 26, 2024. <https://doi.org/10.1038/s41598-020-70816-2>.
- Turner, B. L., Kasperson, R. E., Matson, P. A., McCarthy, J. J., Corell, R. W., Christensen, L., Eckley, N., Kasperson, J. X., Luers, A., Martello, M. L., Polsky, C., Pulsipher, A., and Schiller, A. 2003. "A Framework for Vulnerability Analysis in Sustainability Science." *Proceedings of the National Academy of Sciences*, 100(14): 8074–8079. Accessed December 26, 2024. <https://doi.org/10.1073/pnas.1231335100>.

- U.S. Army Corps of Engineers. Hydrologic Engineering Center River Analysis System. Accessed December 26, 2024. <https://www.hec.usace.army.mil/software/hecras/>.
- U.S. Army Corps of Engineers. RAS Mapper. Accessed December 26, 2024. <https://www.hec.usace.army.mil/confluence/rasdocs/rasum/latest/viewing-results/inundation-mapping-with-hecras-mapper>
- U.S. Army Corps of Engineers. HEC-GeoRAS. Accessed December 26, 2024. <https://www.hec.usace.army.mil/software/hec-georas/>.
- U.S. Department of Transportation (USDOT). (n.d.) *Federal Flood Risk Management Standard*. Accessed December 26, 2024. <https://www.transportation.gov/priorities/climate-and-sustainability/transportation-flood-risk>.
- U.S. Geological Survey. Flood Inundation Mapping Program. Accessed December 26, 2024. <https://www.usgs.gov/mission-areas/water-resources/science/flood-inundation-mapping-fim-program>.
- Ussyshkin, R. V., Theriault, L., Sitar, M., and Kou, T. 2011. "Advantages of Airborne LiDAR Technology in Power Line Asset Management." *2011 International Workshop on Multi-Platform/Multi-Sensor Remote Sensing and Mapping*, 1–5. Accessed December 26, 2024. <https://doi.org/10.1109/m2rsm.2011.5697427>.
- Wang, G., Joyce, J., Phillips, D., Shrestha, R., and Carter, W. 2013. "Delineating and Defining the Boundaries of an Active Landslide in the Rainforest of Puerto Rico Using a Combination of Airborne and Terrestrial LIDAR Data." *Landslides*, 10(4): 503–513. Accessed December 26, 2024. <https://doi.org/10.1007/s10346-013-0400-x>.
- Wang, Z., Lai, C., Chen, X., Yang, B., Zhao, S., and Bai, X. 2015. "Flood Hazard Risk Assessment Model Based on Random Forest." *Journal of Hydrology*, 527: 1130–1141. Accessed December 26, 2024. <https://doi.org/10.1016/j.jhydrol.2015.06.008>.
- Wing, O. E. J., Lehman, W., Bates, P. D., Sampson, C. C., Quinn, N., Smith, A. M., Neal, J. C., Porter, J. R., and Kousky, C. 2022. "Inequitable Patterns of US Flood Risk in the Anthropocene." *Nature Climate Change*, 12(2): 156–162. Accessed December 26, 2024. <https://doi.org/10.1038/s41558-021-01265-6>.
- Williams, K., Olsen, M., Roe, G., and Glennie, C. 2013. "Synthesis of Transportation Applications of Mobile LIDAR." *Remote Sensing*, 5(9): 4652–4692. Accessed December 26, 2024. <https://doi.org/10.3390/rs5094652>.
- Xu, H., Ma, C., Lian, J., Xu, K., and Chaima, E. 2018. "Urban Flooding Risk Assessment Based on an Integrated K-means Cluster Algorithm and Improved Entropy Weight Method in the Region of Haikou, China." *Journal of Hydrology*, 563: 975–986. Accessed December 26, 2024. <https://doi.org/10.1016/j.jhydrol.2018.06.060>.

- Young, A. P., Olsen, M. J., Driscoll, N., Flick, R., Gutierrez, R., Guza, R., Johnstone, E., and Kuester, F. 2010. "Comparison of Airborne and Terrestrial LiDAR Estimates of Seacliff Erosion in Southern California." *Photogrammetric Engineering & Remote Sensing*, 76(4): 421–427. Accessed December 26, 2024. <https://doi.org/10.14358/pers.76.4.421>.
- Yue, Y., Gouda, M., and El-Basyouny, K. 2021. "Automatic Detection and Mapping of Highway Guardrails from Mobile LiDAR Point Clouds." *2021 IEEE International Geoscience and Remote Sensing Symposium (IGARSS)*. Accessed December 26, 2024. <https://doi.org/10.1109/igarss47720.2021.9553055>.

Appendix: User Manual of the Missouri Automated Culvert Analysis Tool (MoACAT) Plugin

Introduction

This document provides a step-by-step guide for installing and using the Missouri Automated Culvert Analysis Tool QGIS Plugin (MoACAT). QGIS is a free, open-source GIS software that has gained popularity among GIS users, and it is compatible with various operating systems, including Linux, Unix, Mac, and Windows. Part 1 details the system requirements and guides the user through the installation process, including prerequisites. Part 2 steps the user through a tutorial using the provided datasets packaged with the plugin. Please note that the plugin may require administrative privileges on your machine, and you may need to run AGIS as an administrator to function properly.

Part 1

System Requirements

MoACAT runs within QGIS and depends on the WhiteBoxTools processing algorithms delivered with MoACAT as a QGIS plugin and associated executables. Neither QGIS nor WhiteBoxTools has published system requirements; for both programs and the MoACAT plugin, the system requirements depend on the needs of the user and the size of the data being processed. However, the tool was developed and tested on a system with the following specifications.

Table A-1 System Specifications

Processor	6 core 2.6 GHz base speed.
RAM	64 GB running at 2667 MT/s
Hard Disk	2TB NVMe, M.2, read speeds up to 2500MB/s
GPU	CPU Integrated
Operating System	Windows 11

These specifications are a good starting point for recommended system specifications. In general, with geospatial applications the more RAM and the faster the RAM, the better.

Single CPU core speed is important, and multi-core CPUs are helpful. A high-speed solid state hard drive is strongly recommended. A GPU is not necessary and adds no real benefits.

Required Inputs

The tool requires the following four inputs to predict culvert locations and attributes—one vector layer and three raster datasets:

1. **Road lines vector layer.** The roads layer should include only the roads for which the user is interested in determining culvert crossings. Ideally, this layer is preprocessed by filtering the MoDOT highway database or TIGER roads to the area of interest and road type. Attributes other than a Feature ID (FID) are not required. However, the user can choose any additional attributes to include in this and the final culvert points layer.
2. **Lidar Digital Elevation Model (DEM) raster.** Lidar should ideally be provided at a 2-meter resolution. If a relatively small area of interest is being processed, a 1-meter resolution DEM may be useful for increasing the accuracy of results. The maximum useful resolution that should be considered is 10 meters.
3. **Curve number raster.** A curve number layer with state-wide coverage indicating much runoff is likely to occur from a specific area based on its land cover, soil type, and moisture conditions has been provided with the tool. In addition, a state-wide SSURGO soil hydrologic soil group classification raster and NLCD landcover raster are also included, which may be used to adjust the curve number values for a given grid code.
4. **Rainfall point depth raster.** Atlas 14 rasters are included with the tool. The default design storm for rating is a 24-hour, 100-year storm.

Installation Guide

Step 1: Install QGIS from the included LTR installation executable in the prerequisites folder or from [here](#). Select the Latest Version (Figure A.1). The Long Term Version will be more stable, while the Latest Version will have the most up-to-date features.

Step 2: Open QGIS. From the Plugins menu, select Manage and Install Plugins... (Figure A.2).

Step 3: From the Plugins window, select Install from Zip, browse to the MoACAT plugin zip file, and click on Install Plugin. If you receive the security warning shown (Figure A.3), select Yes.

Step 4: Wait until to receive a message that the installation is successful. At this point, the MoACAT plugin and the WhiteBoxTools plugin should both be installed. Click on Installed.

Step 5: In the plugins menu, make sure both the Automated Culvert Analysis Workflow plugin and the WhiteboxTools for QGIS plugin are installed and checked (Figure A.4). If the box next to the plugins is not checked, click the box to activate them. Close the Plugin pop-up window.

Step 6: From the settings menu, select options (Figure A.5).

Download QGIS for your platform

This page provides binary packages (installers).

The current version is QGIS 3.40.0 'Bratislava' and was released on 2024-10-25.

The long-term builds currently offer QGIS 3.34.12 'Prizren'.

QGIS is available on Windows, macOS, Linux, Android and iOS.

Long Term Version for Windows (3.34 LTR)

Latest Version for Windows (3.40)

The OSGeo4W Installer is recommended for regular users or organization deployments. It allows to have all components in one place, and to keep each component up-to-date individually without having to download the whole package.

OSGeo4W Network Installer

Since QGIS 3.20 we only ship 64-bit Windows executables.

Figure A.1. QGIS Install



Figure A.2. Plugins Menu

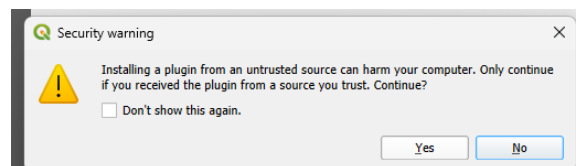


Figure 3. Security Warning

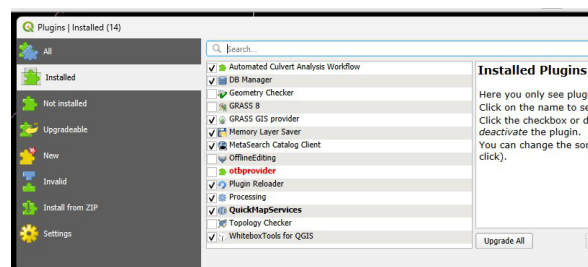


Figure 4. Installed Plugins

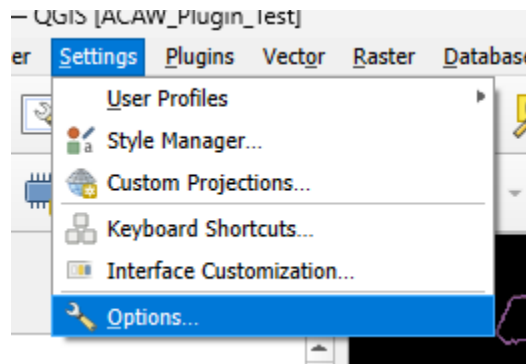



Figure 5. Settings Menu

Step 7: From the Options menu, select Processing>Providers>WhiteboxTools, then make sure "whitebox_tools.exe" is selected and click on OK. Otherwise, click on the WhiteboxTools executable to have an ellipsis mark with three dots to locate the whitebox_tools.exe file (Figure A.6) you extracted from the WhiteboxTools.zip in Step 2. The file may be under a hidden folder

(e.g., \\Users\\username\\AppData\\Roaming\\QGIS\\QGIS3\\profiles\\default\\python\\plugins\\automated_culvert_analysis_workflow\\WBT).

Now, you should be able to see the Automated Culvert Analysis Workflow tool (). The plugin should now be fully installed. If not already visible in QGIS, type CTRL+ALT+T to activate the Processing Toolbox (Figure A.7).

The Automated Culvert Analysis Workflow toolbox should be visible. If not, you can search for it by typing in "Automated" to make it appear at the top.

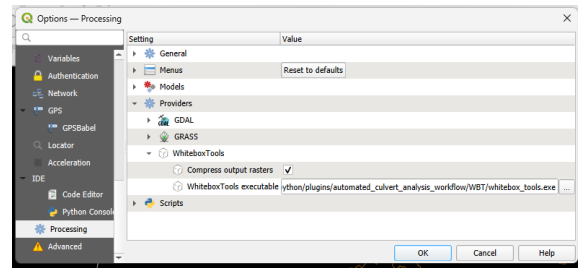


Figure A.6. WhiteboxTools Executable

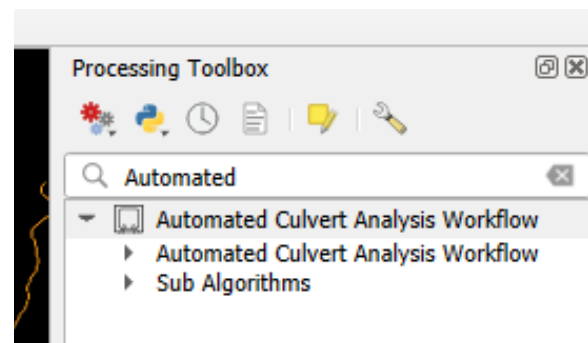


Figure A.7. MoACAT Processing Toolbox

Part 2 Example Walkthrough

Once the plugin is installed, go first to the Plugins Menu and select the Automated Culvert Analysis Tool (Figure A.8). Click on it to open the dialog box. Once the dialog box appears, click OK (Figures A.9 and A.10). This will complete the setup of the WhiteboxTools plugin and load the example data.

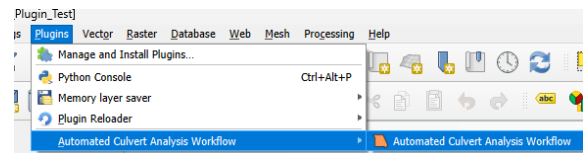


Figure A.8 MoACAT Plugin Menu

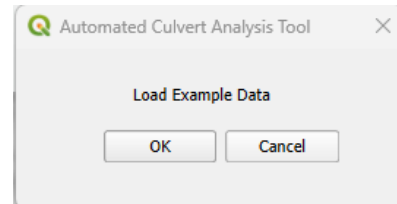


Figure A.9 ACAT Dialog Box

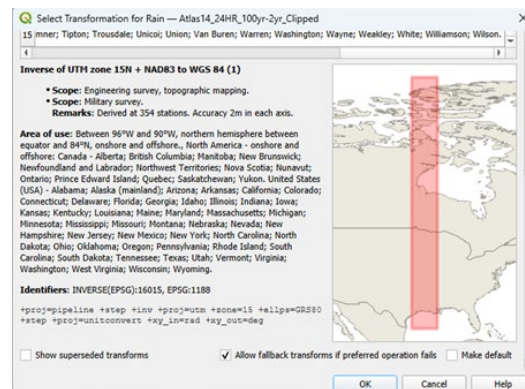


Figure A.10 Datum Transformation

Figure A.11 shows what the QGIS window should look like after the example data is loaded.

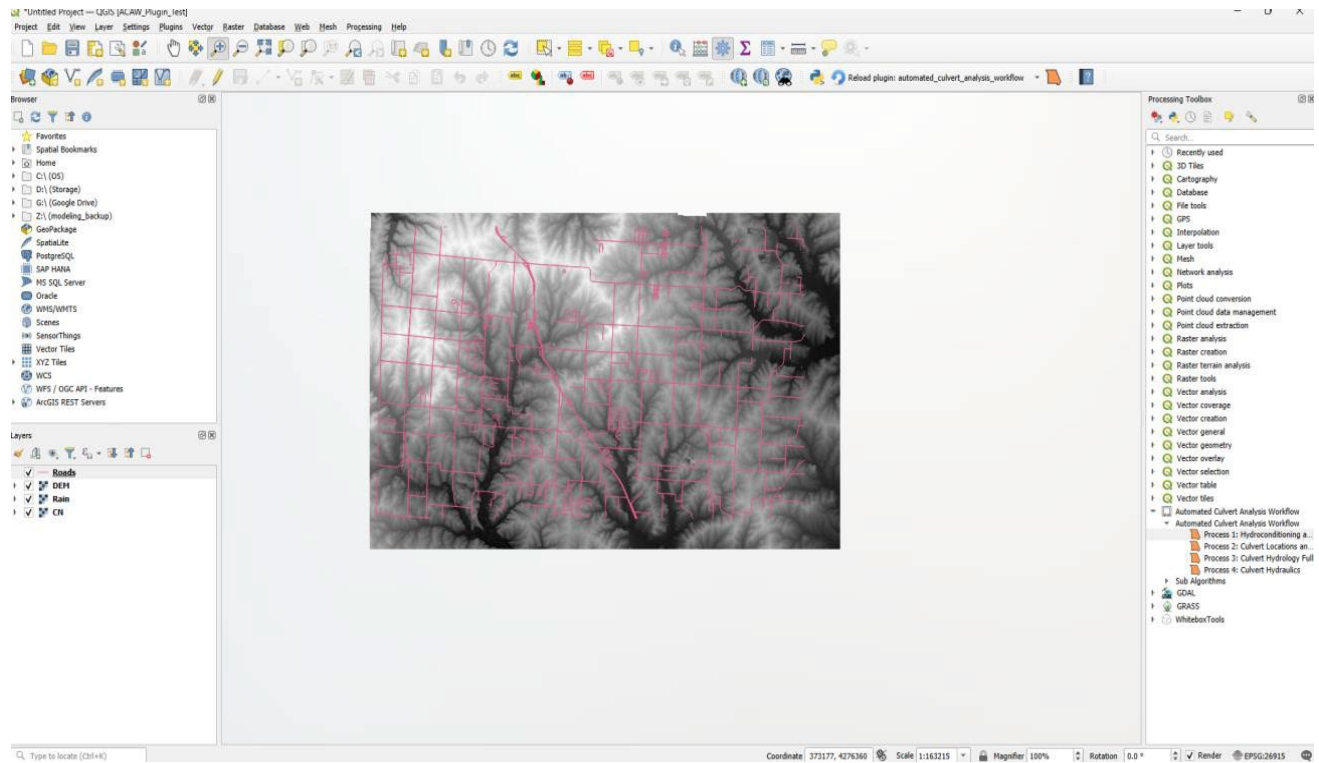


Figure A.11. Example Data in Map Canvas

Processing Tools

Once the software is installed and the example data is loaded, you may begin to use the processing tools. At this point, it is a good idea to save your project, which you can do by typing CTRL+S or by clicking on the save icon (Figure A.12).

To begin the processing workflow, navigate to the Processing Toolbox and select Process 1: Hydroconditioning and Stream Creation (Figure A.13). The sections below will describe how to use each of the processing tools.

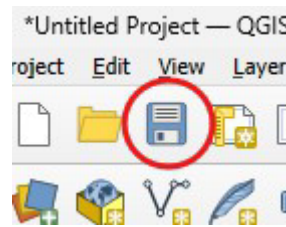


Figure A.12. Save Icon

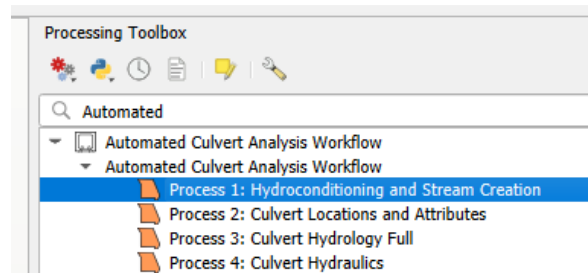


Figure A.13. Process 1 Toolbox

Process 1: Hydroconditioning and Stream Creation

The Process 1 model interface to customize parameters is shown in Figure A.14 below. The right window describes each tool and each of the parameters. Choose the DEM layer in the Input DEM Layer drop-down menu. Set the SEARCH DISTANCE to 25, the Maximum Breach Cost to 15, and the Channelization Threshold to 200000. Leave all the outputs set to *[Save to temporary file]*. Click on Run to start running the tool.

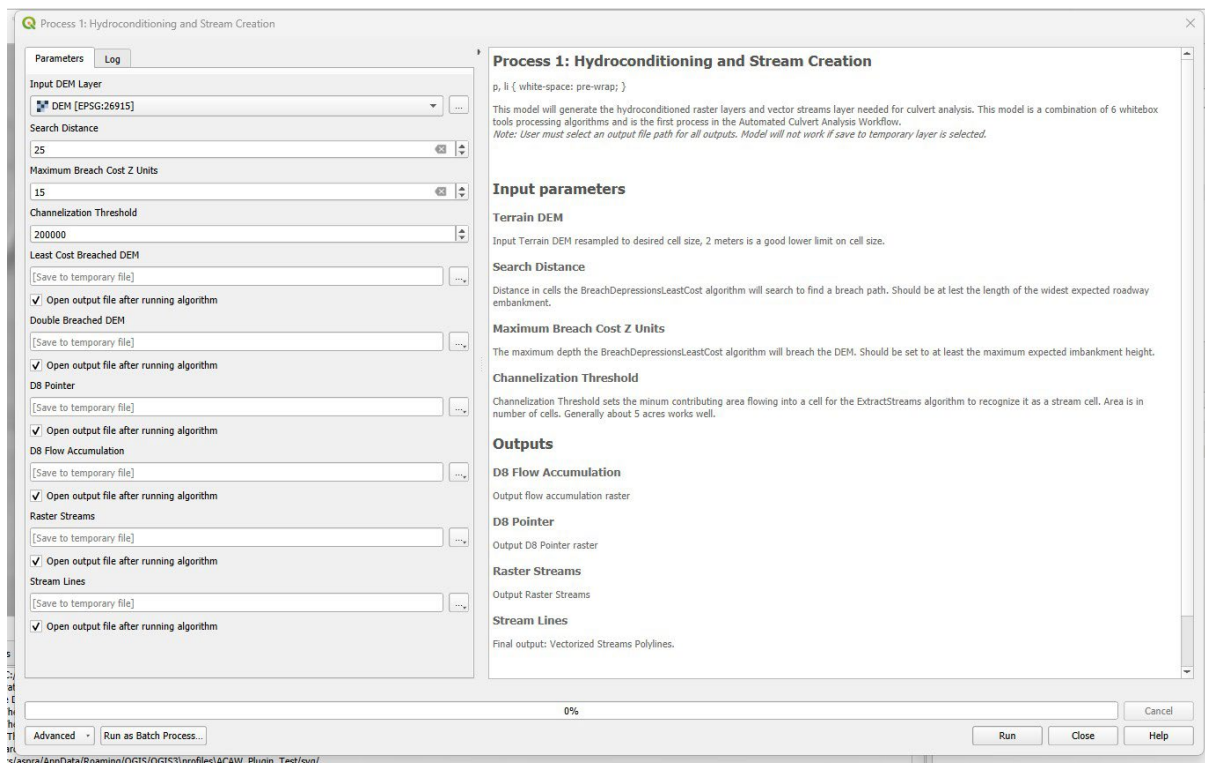


Figure A.14. Process 1 Tool

After the tool has finished running, you should see the following layers added to the project in your layers panel (15):

- Raster Streams
- Double Breached DEM
- D8 Flow Accumulation
- Stream Lines
- Least Cost Breached DEM
- D8 Pointer.

Right-click on the Stream Lines layer, scroll to Layer CRS, and select Set to EPSG:2615, as shown in Figure A.16.

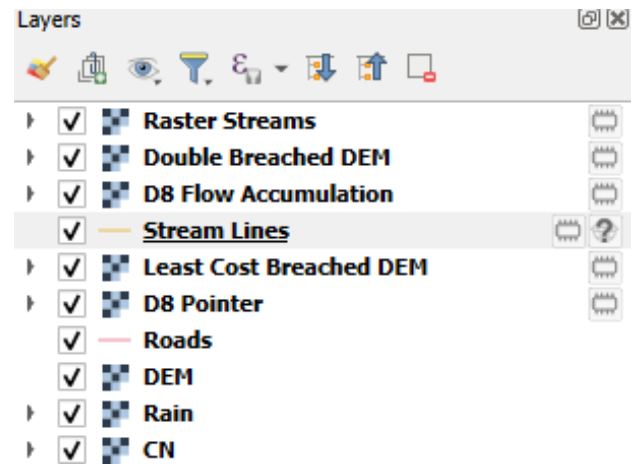


Figure A.15. Process 1 Layers

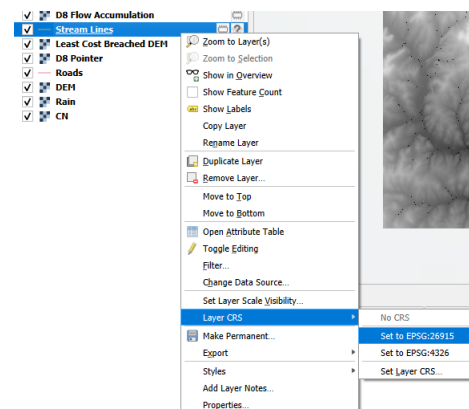


Figure A.16. Layer CRS

Then, right-click on the Stream Lines layer again and select *Move to Top*. You should now be able to see the Stream Lines Layer, and your map canvas should look similar to Figure A.17 below.

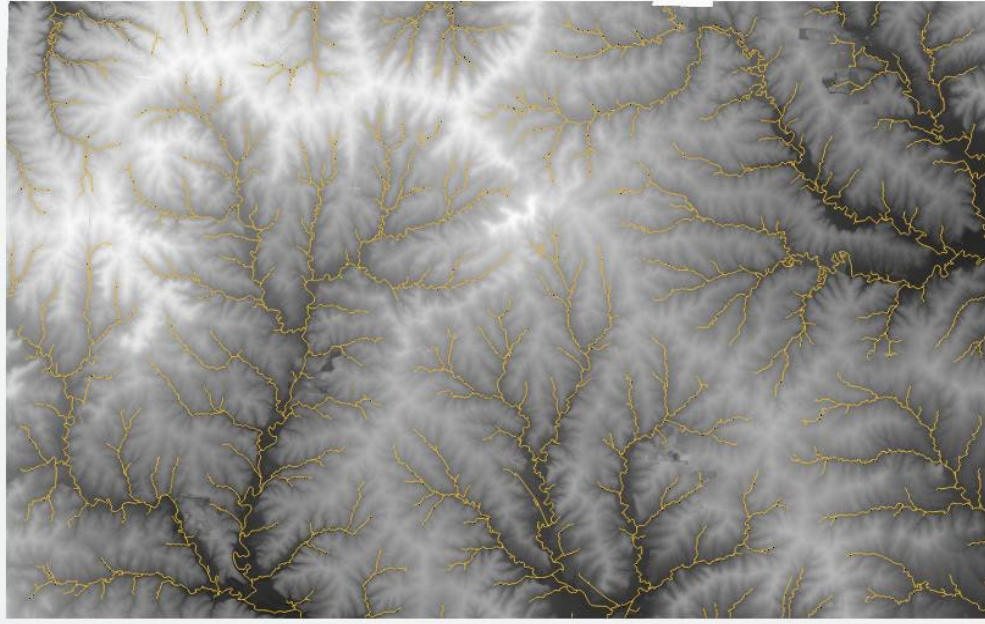


Figure A.17. Stream Lines

Save the project before moving on to Process 2.

Process 2: Culvert Locations and Elevation Attributes

For Process 2, you will need to select three inputs: the DEM layer, the Roads layer and the Stream Lines layer. You also need to select the culvert buffer distance, which determines how far the algorithm will search for the highest and lowest elevations near the culvert to estimate the invert and crown elevations. The stream buffer distance is used to limit the elevation search to the areas inside the stream banks. The units of the input files in the example are meters. Your Process 2 tool window should look like Figure A.18 below. Once it does, click Run.

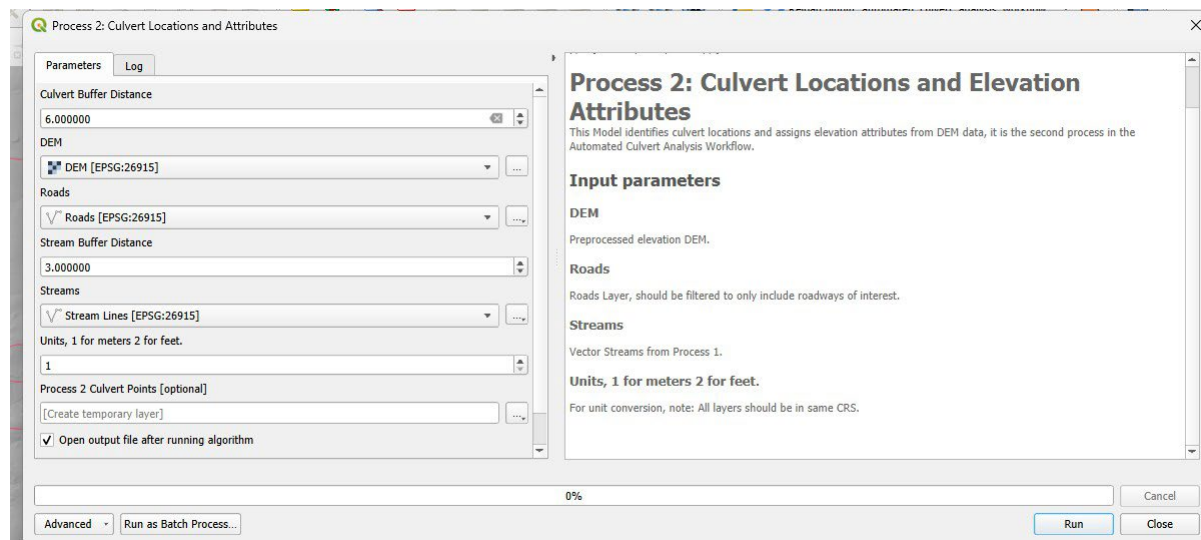


Figure A.18. Process 2

Process 2 will output a point vector layer called Joined layer. If you would like, you may rename this layer to something more descriptive, such as Culverts.

Process 3: Culvert Hydrology Full

For process 3, select the parameter inputs shown in Figure A.19 below. Rainfall Conversion Factor can be left at 1000. If output parameters are left to output to a temporary layer, the tool will output a lines layer called Merged, which contains the longest flow paths for each of the culvert basins. It will also output a point layer called Calculated, containing the culvert points with the added hydrological attributes. It will also output a polygons vector layer called Calculated, which contains the culvert watersheds. Figure A.19 shows the resulting layers in the map canvas and layers panel. If you receive an error, try clicking Advanced, selecting algorithm settings, and setting invalid feature filtering to 'Do not Filter.'

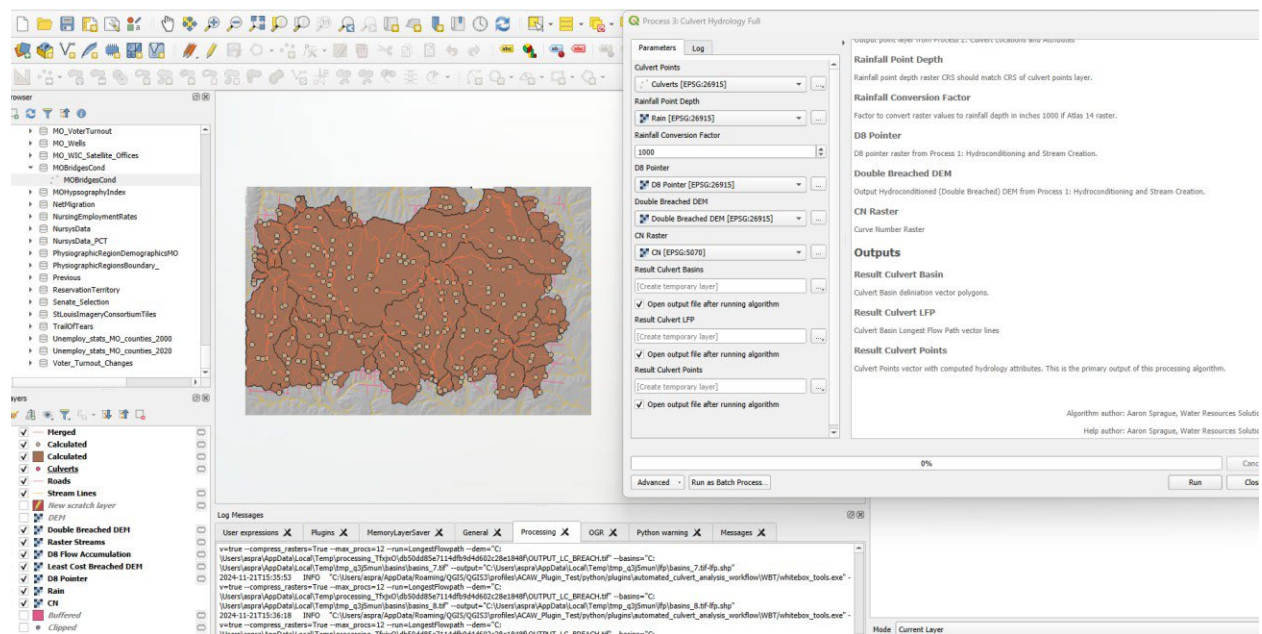


Figure A.19. Process 3

Process 4: Culvert Hydraulics

For the final process, select the Culverts layer created in Process 2 and select the following four attribute fields from the layer in the Process 4 Tool parameters window. The fields to select are as follows:

- Curve Number: b_CN_mean
- Slope of Longest Flow path: L_AVG_SLOPE
- Culvert Basin Area: b_area_ac
- Culvert Design Discharge: Qp

Process 4 will not create a new layer but instead will add attributes and their values to the selected layer. The correct inputs for the example data for the Process 4 Tool are shown in Figure A.20. When the tool has successfully completed running, the log will output the error, as shown in Figure A.21.

This error can be disregarded.

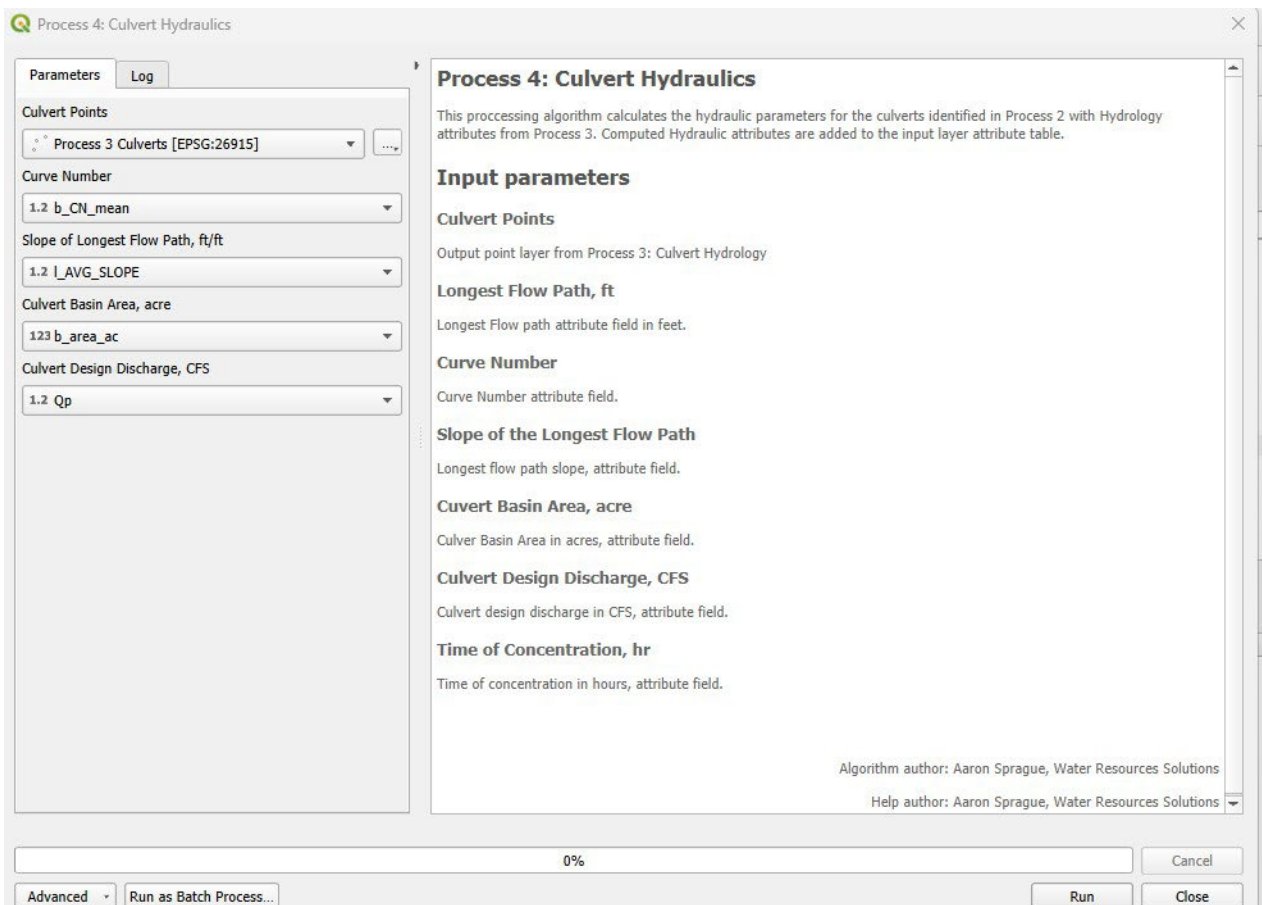


Figure A.20. Process 4

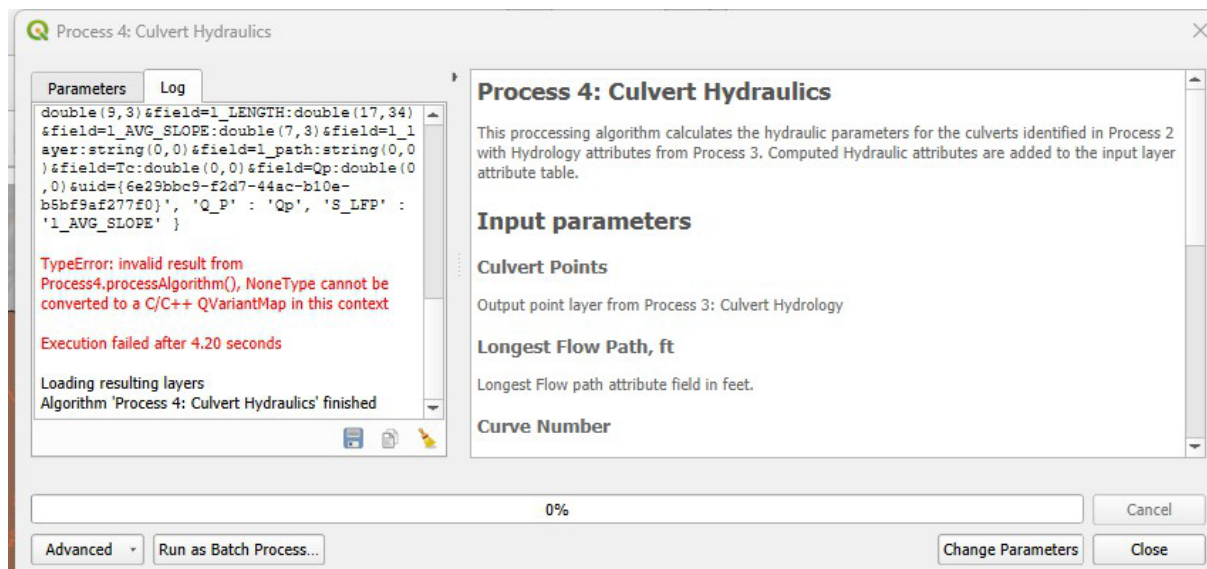


Figure A.21. Process 4 Completion

Final Culvert Layer Attribute Fields

The table below is a list of the attribute fields that the tool generates and uses in calculations. Throughout the process, other attribute fields are also generated and any attributes in the original roads layer from Process 1 remain. However, any Attributes in the final culvert layer that are not listed in the table below and are not attributes from the original roads layer are intermediate attributes that the user can delete if they so choose. A future improvement that could be implemented to the plugin is a tool that removes the intermediate attribute fields and cleans up the remaining attribute names, but this has not yet been implemented at the time of writing.

Table A-2. Culvert Layer Attribute Fields

Field	Description
OID	Unique identifying number for each culvert identified
us_invert	Estimated upstream invert elevation, in raster DEM units
ds_invert	Estimated downstream invert elevation, in raster DEM units
crown	Estimated crown (top of road) elevation, in raster DEM units
prec_depth	Precipitation (rainfall) depth for culvert capacity test storm
b_area_ac	Area of watershed that drains to culvert, in acres
L_LENGTH	Length of longest flow path through culvert watershed, in raster DEM units
L_AVG_SL OPE	Average slope of the longest flow path through culvert watershed, in raster DEM units
Tc	Computed SCS watershed lag method time of concentration for culvert watershed
Qp	Computed culvert capacity test storm peak runoff flow rate, in CFS
Height	Estimated culvert height, in feet
Width	Estimated culvert width, in feet
LS	Estimated drop through culvert
Tw	Estimate tailwater depth
HH	Estimated flow depth for culvert test storm, assuming a culvert of infinite height (Note: If culvert is estimated to overtop disregarded this value, as it doesn't take into account the increased flow capacity that occurs once weir flow over the top of the crown is achieved).
Overtop?	Determination of whether culvert overtops during culvert capacity test storm.